Politecnico di Torino

Corso di Laurea Mechanical Engineering
A.a. 2020/2021
Sessione di Laurea Ottobre 2021

Design of a test bench for the flow ripple determination in positive-displacement hydraulic pumps

Relatori:
Daniela Misul
Miquel Torrent Gelmà

Candidato:
Andrea Gallo

ABSTRACT

This thesis is about the study of two important characteristic values of positive-displacement pumps, the source flow ripple, and the source impedance. The first one represents the flow fluctuations generated inside the pump, while the other one the complex ratio between the pressure fluctuation and the flow ripple occurring at the outlet port of the pump when the Norton model is used. The fluctuations of flow rate are inherent to these types of machines due to their working principle. Moreover, they generate pressure fluctuations in the hydraulic circuit at which the pump is connected and consequently leading to fluid-born noises. By knowing the two mentioned features values and the ripple propagation characteristics of the circuit's components, it is possible then to compute the pressure fluctuations through mathematical models. In such a way, it is furnished the tool to design circuits with low hydraulic noises values.
The main aims of this thesis are the following ones:

- Design a test bench suitable for characterizing pumps of different sizes using three different kits.
- Write a Matlab code to compute the source flow ripple and the source impedance of positive-displacement pumps.
- Test a 10.6 cc/rev external gears pump to prove the correctness of the code and of the methodology followed.

For both the design of the test bench and the drafting of the code it is followed the standard ISO 10767:1-2015.
To design the three kits are taken into account two external gear pumps and an axial piston pump equivalent to SAE-A, SAE-B and SAE-C dimensions according to standard SAE J-744 [1]. In this way it is possible to cover a wide range of pump dimensions.
The Matlab code provides a tool not only for the computation of the characteristic values of the pump but also for a direct verification of the calculations through different mathematical models.
Moreover, for the verification of the methodology, the 10.6 cc/rev pump is tested in the Laboratory of Fluid Mechanics of the "Universidad Politécnica de Cataluña". Here, after analyzing the pump's dimensions, the required test bench is mounted and different tests are carried out.
The experimental results achieved show the typical behaviour of an external gear pump. In addition, they exhibit a good correlation with both mathematical models and scientific articles, validating our calculations.
To sum up, this thesis gives a useful overview of the pump's main characteristics and allows to follow a methodology regarding the design of a test bench suitable to characterize positive-displacement pumps having different dimensions.

Contents

GLOSSARY

Q_{TH} : theorical flow rate
C_v: pump derived capacity
n: rotational speed
z: number of pumping elements
Q_S: source flow ripple
Z_S: source impedance
Q_S^*: source flow ripple (modified model)
Z_C: characteristic impedance
Z_e: entry impedance
P: pressure ripple
β: wave propagation coefficient
ξ: unsteady viscous friction coefficient
P_b: blocked acoustic
R:resistance
F:harmonic
f_{shaft}: shaft frequency
ρ:fluid density
c: speed of sound
E: Young modulus
B: bulk modulus
δ_T: wave reflection coefficient

CHAPTER 1

1.1 OBJECTIVES

The main aims of this thesis are:

- Design a test bench suitable for the determination of the source flow ripple and the source impedance of positive-displacement pumps of different sizes using three different kits.
- Write a Matlab code to compute the previous characteristic values of a positive-displacement pump.
- Test a 10.6 cc/rev external gears pump to prove the correctness of the code and of the methodology followed.

1.2 SCOPE

To design a test bench suitable for pumps with different dimensions and working principles two external gear pumps and an axial piston pump are taken into consideration. Thus, three different kits suitable for the test bench are designed covering a wide range of pump's dimensions.
Then a Matlab code is written to compute the source flow ripple and the source impedance of the pumps. In addition, the code contains a comparison with mathematical models to understand the quality of the results obtained from the experimental tests.
To design the test bench and to write the code the standard ISO 10767:1-2015 is followed. Moreover, a test bench is mounted in the Laboratory of Fluid Mechanics of Universidad Politécnica de Cataluña. In this way, by testing a 10.6 cc/rev external gear pump it is possible to prove if the Matlab code and the methodology followed to design the test bench are reliable.
The pump is tested in various working condition, at 50, 75 and 90 bar. In this way, it is also possible to understand if the source flow ripple and the source impedance are influenced by the working pressure. Afterwards, the experimental results obtained are compared with the theoretical models and with scientific articles. Thus, a direct tool to understand the reliability of our code and the methodology followed is furnished.

1.3 REQUIREMENTS

To design properly the test bench, it is required the study of the standard ISO 10767:1-2015. By doing so, it is possible to understand the influence of the pump's dimension on the various components that make up the three kits.
Furthermore, it is necessary the knowledge of the software Matlab and Excel. The first one to write the code while the second to process the experimental data provided by the digital scope used to sample the pressure fluctuations.
In addition, to obtain the desired results it is required a basic study of propagation of fluctuations in the hydraulic pipes, focusing on the standing waves. Afterwards, the analogy between the hydraulic circuit and the AC current is considered to simplify the calculations and to obtain a straightforward model. Finished the theorical part, the required test bench is mounted in the Laboratory of Fluid Mechanic of UPC university. At this regard, it is used instrumentation easily available in the Fluid Dynamics Department of UPC University without the need of buying anything new, exploiting also obsolete equipment like the digital scope.

1.4 JUSTIFICATIONS

The pressure ripple due to flow rate fluctuations generates vibrations and airborne noises inside the hydraulic circuit. This aspect can be very critical. Therefore, to improve the design of circuits and to choose the more appropriate hydraulic pump is fundamental the computation of the source flow ripple and the source impedance. Knowing these two parameters it is possible to understand pump's noise generating potential. Moreover, if it is known also the ripple propagation characteristics of the components of the hydraulic circuit, the pressure fluctuations can be computed using specific software. In this way, a complete analysis of the circuit is obtained. Thus, it is easy to understand the necessity of designing a test bench suitable for the characterization of different positive-displacement pumps. Furthermore, this thesis brings an innovative aspect to UPC university since until now there was only experience with the previous standard.
This thesis is developed in eleven chapters which are divided as follow:

- Chapter 2 explains briefly the flow fluctuations generated in a positive-displacement pump.
- Chapter 3 explains the theory of waves propagation inside pipes, focusing on standing waves and on the analogy of pump's impedance with the AC current.
- Chapter 4 contains a comparison between the ISO Standards published in 1996 and in 2015, focusing on how the methodology has been simplified during the years, but also in the negative aspects of the current standard.
- Chapter 5 contains the description of the designed test bench with its drawing and the explanation of the methodology to follow.
- Chapter 6 embodies a description of the test bench installed in the Laboratory of Fluid Mechanics of UPC university.
- Chapter 7 includes the various tests carried out and the respective validations comparing the results obtained with mathematical models.
- Chapter 8 contains a comparison of the results with scientific articles.
- Chapter 9 includes the budget and the economic viability of our tests.
- Chapter 10 explains the environmental impact of the tests.
- Chapter 11 includes the conclusions and future work proposals.

CHAPTER 2:

FLOW RIPPLE GENERATION IN POSITIVE-DISPLACEMENT PUMPS

Depending on their working principles hydraulic pumps can be classified in two main categories, rotodynamic pump, where a rotary element called impeller imparts energy to the fluid, and positive-displacement pump. The first class is used when the main goals are working with high flow rates and low pressures, while positive-displacement pumps are applied when is required to work with high pressures and low flow rates. The latter type of pumps can additionally be divided in different sub-categories and the most important are rotatory and reciprocating pumps. Their common characteristic is that under ideal condition the flow rate generated depends only on the rotational speed and on the pump derived capacity ($Q_{th} = n \cdot c_v$). Where the latter characteristic is defined as the volume of fluid delivered at each working cycle. Consequently, compared to turbomachinery, the flow rate is not affected by the working pressure.

2.1 FLOW FLUCTUATIONS

The main disadvantage of positive displacement pumps is related to the delivered flow rate since it fluctuates over time and consequently causes vibrations and noises in the hydraulic circuit. The flow ripple is caused by their working principle. During their working cycle, the pumping elements (such as pistons, gear teeth or vanes), deliver a volume of fluid that in time can be described as half sine wave. Summing altogether the different flow contributions is found a variable trend over time.

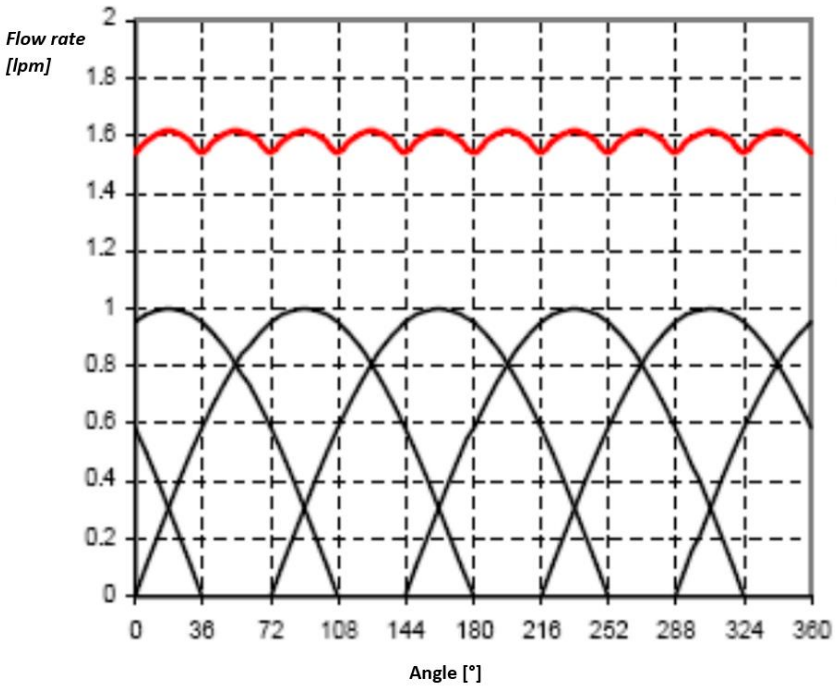

Figure 1 Instantaneous flow rate of an axial piston pump

As we can see in figure 1 the flow ripple is periodic with a frequency equal to $\frac{nz}{60}$ where n is the rotational speed of the prime mover and z the number of working elements. Depending on the type of positive displacement pump, the fluctuations may strongly depend on the

working pressure. In case of axial piston pumps in addition to the working principle, the flow ripple depends on external conditions. During the rotation of the pistons around the swash plate, in the delivery phase the fluid sees a pressure difference respect the outlet port. The pressure variation respect to the discharge port leads to the fluid compression that causes a back flow and thus a further fluctuation on the flow delivered. On the other hand, in case of external gear pumps the contribution of the pressure is negligible respect to the working principle. Consequently, only the geometry of the pump generates the flow fluctuations leading to a behaviour more easily predictable. Thus, following the theorical approach proposed by Johnston [2], the fluctuations of flow for an external gear pump between the angular width $-\frac{\pi}{z} < \psi < \frac{\pi}{z}$ is evaluated as:

$$Q(\psi) = Q_{max} - K\psi^2 \qquad (1)$$

Where the coefficient K depends on the type of gear teeth, involute or cycloidal, the gear width b, the angular velocity of the gears ω, the radius of the pitch circle and the pressure angle θ:
$K = b\vartheta r^2 cos^2\theta$ for involute gear teeth
$K = b\vartheta r^2$ for cycloidal gear teeth.
Moreover, the flow rate irregularity is defined as:

$$\sigma = \frac{\mathrm{Q_{max}} - \mathrm{Q_{min}}}{\mathrm{Q_{mean}}} \qquad (2)$$

CHAPTER 3

WAVE PROPAGATION IN PIPES:

In the analysis of the flow and pressure ripple in hydraulic circuits it is important focusing on how the propagation of fluctuations is carried out in pipes. Consequently, it is preferable to examine these phenomena by using the plane wave theory.

3.1 PLANE WAVES

Plane waves are a sub-category of waves whose main characteristic is that they are spatially unidimensional, thus, the vector field transferred is invariant over a plane perpendicular to the propagation's direction. Therefore, if we consider the z axis as the direction of motion of the wave, the vector field will be uniform in x and y direction.

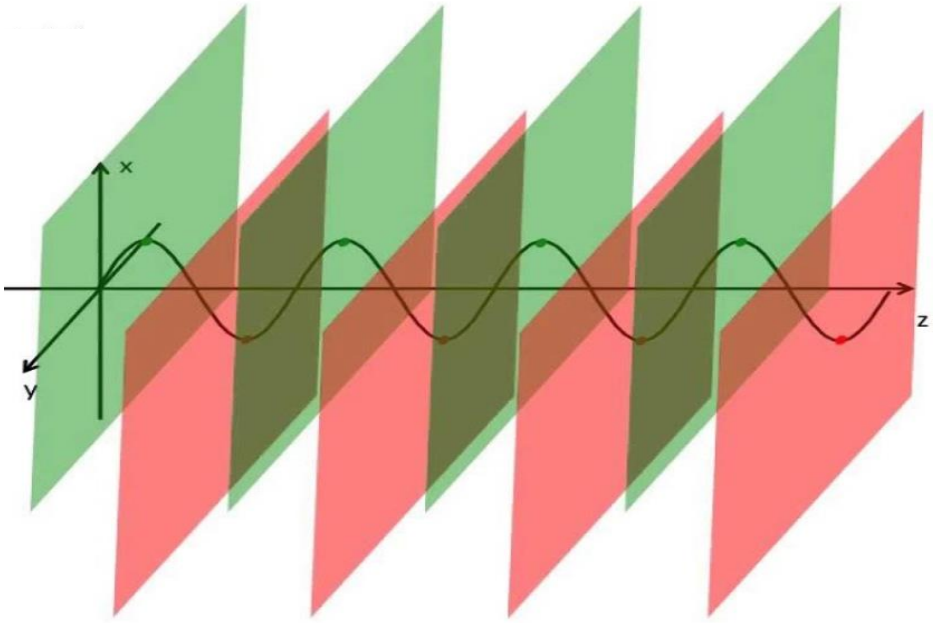

Figure 2 Sinusoidal plane wave

Even if plane waves are a physical idealization, they are a powerful tool to understand and to explicate the behaviour of certain phenomena. For example, when we analyze a point wave source, we can see that it produces spherical waves which when they are examined far away from its source can be approximate with plane waves. Consequently, plane waves can be used without adding a significative error.

3.2 REFLECTION

Important aspects to consider are the phenomena of reflection and refraction. When a wave during its propagation sees a change of medium, two new waves occur. The first one called the reflection, is a wave whose direction is opposite to the incident one, while the second is the refraction wave whose propagation occurs in the second medium. Due to the relationship ($\lambda = v/f$) we easily understand that if during the change of the medium the refraction wave changes velocity of propagation, it also changes its wavelength. But when, as well as in our case study, the wave is harmonic since the source remains constant the frequency *f* and the radial frequency ω will not vary.

In our study, the hydraulic circuit is not homogenous, but different variations are present. For example, the presence of components like valves and hydraulic fittings change the pipeline's cross section. For this reason, we have also to consider the formation of reflection waves, which in turn will lead to the generation of other partial reflections. This phenomenon will repeat itself in time leading to the interference of waves propagating with same frequency but in opposite directions. Consequently, standing waves will be formed [3].

3.3 STANDING WAVES

Now it is useful to understand the behaviour of standing waves in hydraulic circuits. Firstly, we take into account the simple case of pipelines and later we will consider an entire circuit. For the first case, two possibilities can occur. The case of a pipeline with a closed end section which is characterized by the presence of a node in the closed section and an antinode in the open section. And the case of a total opened pipe where there are antinodes at the two ends of the pipe. It is remembered that a node is characterized by a wave amplitude's value equal to zero, while an antinode is characterized by a maximum value of the amplitude. The two cases do not differ only for the position of the antinodes, but also for the values of the harmonics.

- Both ends opened:

The first harmonic, which is called also the fundamental one, has only one node and its wavelength is equal to two times the length of the pipe. The following harmonics are multiple of the first one and will follow the relationship:

$$f_{k-th} = \frac{k \cdot v}{2 \cdot L} \qquad (3)$$

- One end section closed:

Since in this case the geometry is asymmetric the harmonics that can be found must satisfy the following condition:

$$f_{k-th} = \frac{k \cdot v}{4 \cdot L} \qquad (4)$$

where k is an odd integer. Consequently, the fundamental harmonic has a wavelength equal to four times the length of the pipe and the k-harmonics will follow the relationship $f_{k-th} = k \cdot f_{1st}$ with k=1,3,5,7…

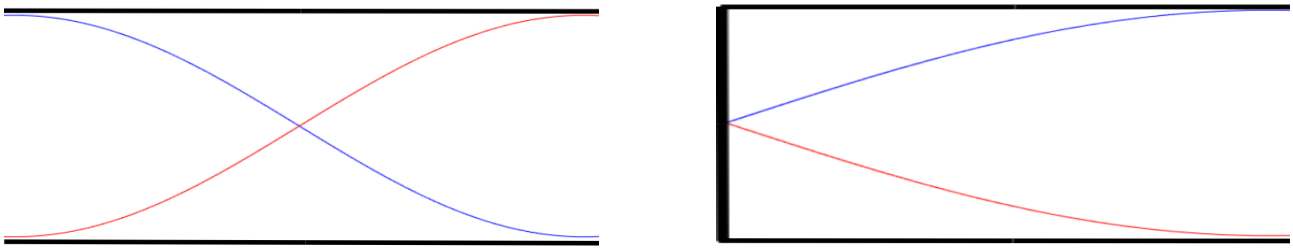

Figure 3 Fundamental harmonic both ends opened and one end closed

Now it is easily understandable how a hydraulic circuit can influence the behaviour of the pressure ripple and how due to the presence of nodes and antinodes, belonging to distinct harmonics, it is difficult to obtain a direct measurement of the pressure ripple.

3.4 WAVE'S EQUATIONS

In addition, to evaluate the wave propagation caused by the flow fluctuations it is useful to focus our attention on an infinitesimal portion of the pipe which coordinates are x on the left side and $x + \partial x$ on the right, as explained by Johnston [2].

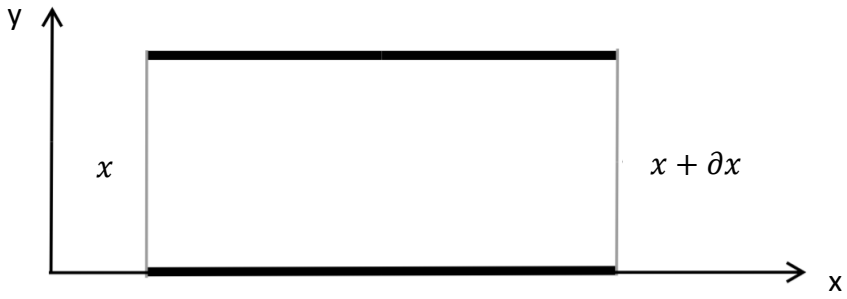

Figure 4 Infinitesimal portion of the pipe

Considering the flow continuity equation:

$$-\frac{\partial q}{\partial x} = \frac{A}{B_{eff}}\frac{\partial p}{\partial t} \qquad (5)$$

and the resultant of the forces on the infinitesimal portion:

$$-\frac{\partial p}{\partial x} = Rq + \frac{\rho}{A}\frac{\partial q}{\partial t} \qquad (6)$$

where p and q are the fluctuations of pressure and flow in the time domain, A the pipe's cross section, B the bulk modulus and R the pipe's resistance. Considering that our aim is to achieve the harmonic spectra, through a Fourier transformation, we achieve the following equations:

$$-\frac{\partial Q}{\partial x} = \frac{A}{B} j\omega P \qquad (7)$$

$$-\frac{\partial P}{\partial x} = \left(R + \frac{j\omega\rho}{A}\right) Q \qquad (8)$$

where $j = \sqrt{-1}$.
Finally, rearranging the equations 7 and 8, the wave equations are computed as explained by Johnston [2]:

$$-\frac{\partial^2 Q}{\partial x^2} = \beta^2 Q \qquad (9)$$

$$-\frac{\partial^2 P}{\partial x^2} = \beta^2 P \qquad (10)$$

where Q, P and β are respectively the flow ripple and the pressure ripple in the frequency domain, while β is the wave coefficient which depends on the angular frequency, the speed of sound, the internal radius of the pipeline and the kinematic viscosity of the test fluid.
Moreover, for both the pressure and flow fluctuations are found the following equations:

$$P(\omega, x) = Fe^{-\beta x} - Ge^{\beta x} \qquad (11)$$

and

$$Q(\omega, x) = \frac{Fe^{-\beta x} - Ge^{\beta x}}{Z_0} \quad (12)$$

where the first term of the equation stands for a wave moving to the right while the second term stands for a wave moving to the left. Additionally, the term Z_0 represents the pipeline impedance which will be later explained.
Now if we consider a hydraulic circuit such as the one of figure 5, we can compute the values of pressure and flow fluctuations. For the boundary condition we take into account that the pump is modelled as an impedance Z_s, in parallel with a source of flow ripple Q_s. Consequently, we achieve as demonstrated by Johnston [2]:

$$Q_S = Q_0 + \frac{P_0}{Z_S} \quad at\ x = 0 \quad (13)$$

$$Z_L = \frac{P_{(x=L)}}{Q_{(x=L)}} \quad at\ x = L \quad (14)$$

Therefore, considering the latter wave equations and the boundary conditions we find the values of pressure and flow fluctuation for a generic x position:

$$P_x = \frac{Q_S Z_S Z_0}{Z_S + Z_0} \frac{e^{-\beta x} + \delta_T e^{-\beta(2l-x)}}{1 - \delta_S \delta_T e^{-2\beta l}} \quad (15)$$

$$Q_x = \frac{Q_S Z_S}{Z_S + Z_0} \frac{e^{-\beta x} - \delta_T e^{-\beta(2l-x)}}{1 - \delta_S \delta_T e^{-2\beta l}} \quad (16)$$

where the first term of the equation considers only the pressure component produced neglecting the reflection phenomenon, while the second term describes the waves travelling in both directions due to the reflection.
The terms δ_T represents the wave reflection coefficient at the termination of the circuit and it is expressed as the ratio between the reflected and the incident waves. On the other hand, δ_S represents the complex ratio between the reflected and the incident waves travelling in the negative direction and evaluated at the discharge port.
A singular condition is found for a null value of the coefficient δ_T. In fact, it means that no reflected waves are formed leading to a constant pressure along the pipeline. While in case of values different from zero, standing waves will appear which cause fluctuations of the pressure amplitude.

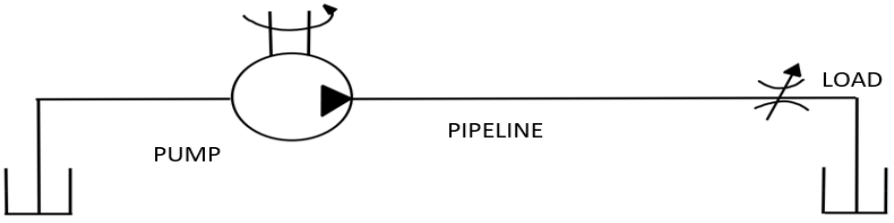

Figure 5 Hydraulic circuit

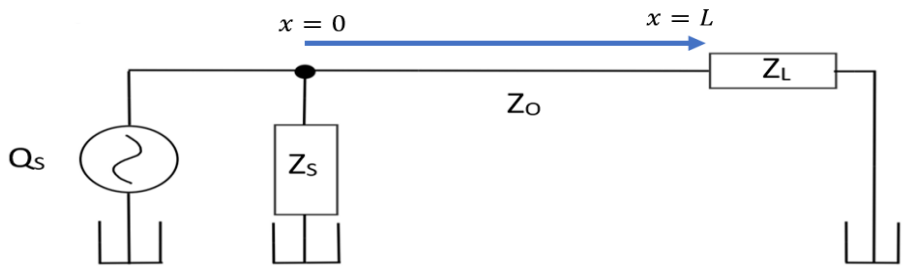

Figure 6 Impedance model

3.5 IMPEDANCE MODEL

As it is possible to understand from the solution of the wave equations, previously explained, and from the example of the simple hydraulic circuit, to better understand the relationship between the fluctuations of both flow rate and pressure, it is required to consider the analogy of the hydraulics with the AC current.
It is remembered that in the electromagnetic field the resistance, the inductor and the conductor are related by the concept of impedance which in Cartesian form it is expressed as

$$Z = R + jX \qquad (17)$$

with the resistance, R, that stands for the real part of the impedance and the reactance, X, that represents the imaginary part. The latter one, additionally, could be a positive value if it represents the capacitor or a negative value if stands for the inductor. Additionally, the impedance, the voltage and the current are related by the formula

$$Z = \frac{|V|}{|I|} e^{j(\Phi v - \Phi I)} \qquad (18)$$

Hydraulic system	Electrical circuit
Volume v	Charge q
Flow rate Q	Current i
Pressure P	Voltage V
Energy=Pressure·Volume	Energy=Voltage·Charge
Power= Pressure· Flow rate	Power=Voltage·Current
ΔPression=Q·Resistance	ΔVoltage=i·Resistance
Flow rate=Capacitance·(dP/dt)	Current=Capacitance·(dv/dt)
Pressure=Inductance·(dQ /dt)	Voltage=Inductance·(di/dt)

Table 1 Hydraulic system-electrical circuit analogy

In the hydraulic field, as seen in table 1, we can also introduce the concepts of resistance, capacitance, and inductance. Therefore, similarly to the AC circuits, we can use the concept of hydraulic impedance which locally represents the ratio between pressure fluctuations and the flow ones.
Different models were developed to study the source impedance of positive displacement pumps and it depends mainly on the following factors:

- Geometry of the pump.
- Fluid property such as density, Bulk modulus and kinematic viscosity.

- Volumetric efficiency of the pump.
- Cavitation phenomenon or liberation of air.

A positive displacement pump can be described in a simple way by a model composed of a resistance and a capacitance in parallel, connected in series with an inductance. In this way, we correlate the resistance with the pressure drop and the leakage's flow rate, the capacitance with the fluid's bulk modulus, and the inductance with the density of the fluid and the geometric characteristic of the hydraulic circuit

$$Z_R = \frac{\Delta P}{Q_{leak}} \quad (19)$$

$$Z_C = -j\frac{\mathrm{B}}{\omega V} \quad (20)$$

$$Z_L = J\omega I \quad (21)$$

with the factor $I = \frac{\rho L}{A}$ which takes into consideration the density of the fluid and the geometry of the hydraulic circuit.
And finally considering the arrangement of the resistance, the capacitance and of the inductance we find:

$$Z_S = \frac{Z_R Z_C}{Z_R + Z_C} + Z_L \quad (22)$$

Other studies such the ones performed by Edge [4] and Davidson [5] found that the source impedance has mainly a capacitive nature affirming that it is equal to:

$$Z_S = \frac{B}{j\omega V} \quad (23)$$

Depending thus on the fluid bulk modulus, on the angular frequency and on the volume of the pump. This model tends to be a good approximation at low frequencies where the inertia of the pump could be neglected but loses its accuracy at higher frequencies. Here the inductance component of the source impedance which takes into account the inertia of the fluid becomes important. To sum up, it is necessary following a different path, such the one described in the Standard ISO 10767 to correctly obtain a more realistic model of the source impedance which can be reliable also at higher frequencies.
Furthermore, the importance of the evaluation of the source impedance is found in the possibility of calculating the pressure ripple and consequently, to understand if the level of noises and vibrations generated overcome requirements or limits imposed by standards and to improve the design of the hydraulic circuit.

3.6 DISCRETE FOURIER TRANSFORMATION

A fundamental mathematical tool in signal processing is the Discrete Fourier transform (DFT). Through this algorithm it is possible to convert a finite signal equally spaced in time into its frequency spectrum. In such a way, it is possible to decompose any signal and so any waveform into its sinusoidal representation in the frequency domain.
Thus, considering a finite time signal $x\,(n\tau)$ with a sampling period τ ,defined as $\frac{1}{fs}$ with fs the sampling frequency and N the number of data sampled, the DFT is defined as:

$$X(i\omega k) = \frac{1}{N}\sum_{n=0}^{N-1} x(n\tau)e^{-j\frac{2\pi nk}{N}} \qquad (24)$$

where:

$$X(i\omega k) = Re[X(k)] + j\, Im[X(k)] \qquad (25)$$

with k=0,1,2,3,….N-1

In our evaluations, we will consider as discrete time signal the pressure fluctuations which occur in the hydraulic circuit. Depending on the maximum frequency of interest, we will choose the most appropriate sampling frequency in accordance with the Nyquist-Shannon theorem. The latter one states that to obtain an accurate reconstruction of an analog signal (continuous) into a digital one (discrete) the sampling frequency must be at least two times the highest frequency of interest. Usually, a good practice is to impose the sampling frequency equal to two and a half time the highest frequency. In fact, if an insufficient number of samples per second are recorded, the nature of the analog signal will be lost, as it is possible to see in figure 7. That is due to the aliasing phenomenon, where high frequency signal during their reconstruction appears as low frequency one.

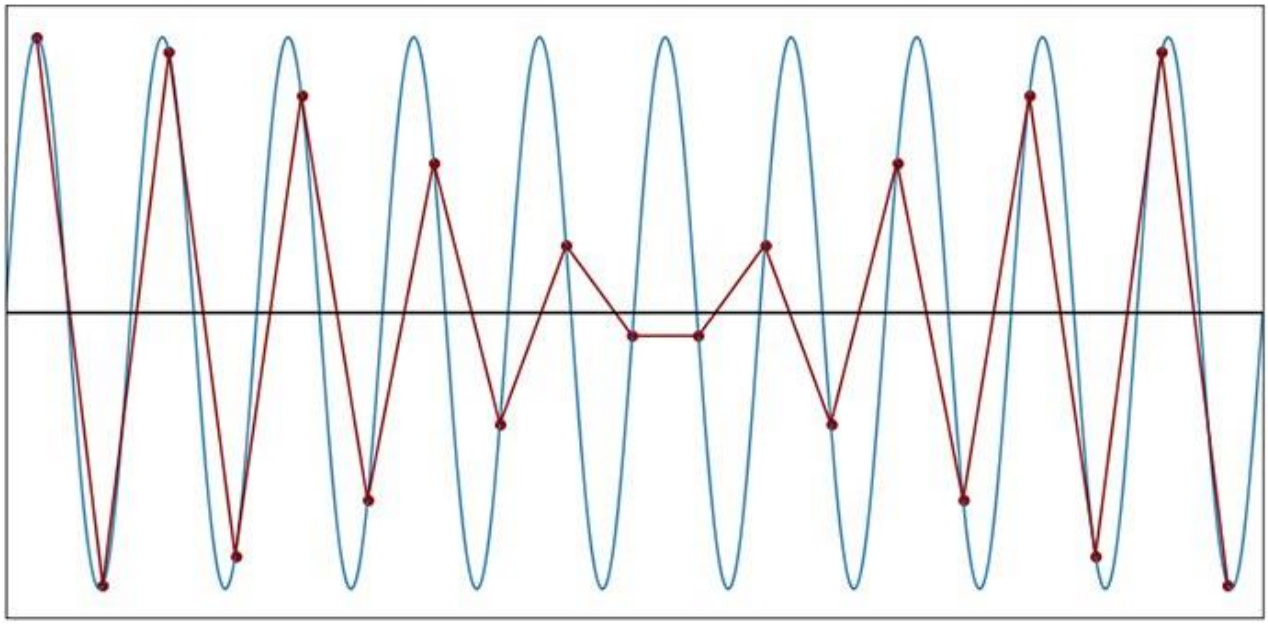

Figure 7 Reconstruction of a sinusoidal signal using a sample rate equal to 1.9 time the sinusoidal frequency

CHAPTER 4:

COMPARISON BETWEEN ISO 10767-1:1996 AND ISO 10767-1:2015

Vibrations and air-borne noises generated by coupling positive-displacement pumps with hydraulic circuits have always been important problems for the industrial fields for both the healthy security of the workers and the efficiency of the machines. Consequently, a need to analyze in a standardized manner the source flow ripple and the source impedance of hydraulic pumps was required making possible the system's malfunctions reduction and the proper selection of pumps.
During the years different mathematical approaches have been used to calculate these parameters and the ISO Standards between the 1996 and 2015 have significantly improved the accuracy and the easiness of calculations.

4.1 ISO 10767-1 1996 EDITION

The first ISO standard was published in 1996 relying on the studies developed in the university of Bath, whose theorical fundamentals are the one-dimensional wave propagation in hydraulic pipes and the impedance analogy with the AC current. Moreover, this standard is also called "the secondary source method" [6] since it makes use of a secondary source to impose an additional pressure ripple source to have enough data to estimate the pump source impedance. The secondary source's task is thus, to supply periodic waveforms whose frequencies cover a range from the pumping frequency to at least ten times its value. To comply with these functions as secondary source can be used another positive-displacement pump, such as a piston one, an electromechanical vibrator with a piston arrangement or a bleed valve. Moreover, in the test rig a ball valve is required to close, when it is necessary, the part of the circuit connected with the secondary source.

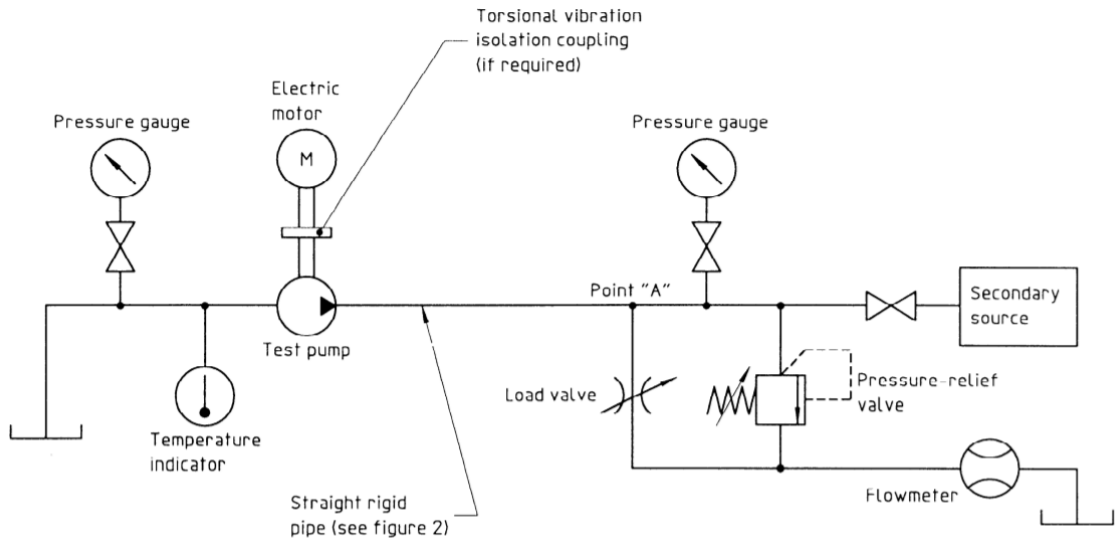

Figure 8 Hydraulic circuit

The use of the secondary source makes this standard difficult to use. In fact, initially the pump's source impedance is computed using the secondary source's frequencies. Consequently, it is necessary to convert the frequencies used for the computations to the pump frequencies through a mathematical model. In this way, the difficulty of the algorithm

to follow is increased. Moreover, the accuracy of the test could be influenced negatively. In addition, this standard depends on the knowledge of the fluid's bulk modulus proposing two different mathematical paths to follow.
Despite the negative aspects, it is important to remember the theoretical basis proposed in this standard. Two mathematical models of the source impedance are proposed, the *distributed* and the *lumped parameter*. They differ by the representation of the outlet port of the positive-displacement pump.
The first model is used when the size of the pipe's outlet pathway is comparable with the wavelength of the harmonics and so the impedance cannot be modelled as a single point.
The second model is used when the wavelength is sufficiently bigger than the physical element considered so that it is possible to model the pump impedance as a single point.

4.2 ISO 10767-1 2015 EDITION

In 2015 the ISO Standard has proposed another methodology to evaluate the source flow ripple and the source impedance of pumps. The research from the university of Bath were discharged and the studies of both Weddfelt and Kojima [7] were followed.
The theory followed by the standard regards, as in the previous version, the unidimensional wave propagation but now another approach is observed.

4.2.1 METHODOLOGY

In this standard two different models are followed to describe the pump's pulsation source. The first one is the Norton model. Here the pump is described as a flow ripple generator in parallel with its impedance, both located at the outlet port of the pump. The second model is called the modified and provides a more realistic representation of the pulsation source since it is located in the inner part of the discharge line. In addition, two sets of tests are required to obtain the characteristics of the pump and for this reason this standard is also called the "two pressures/two systems method" [7].

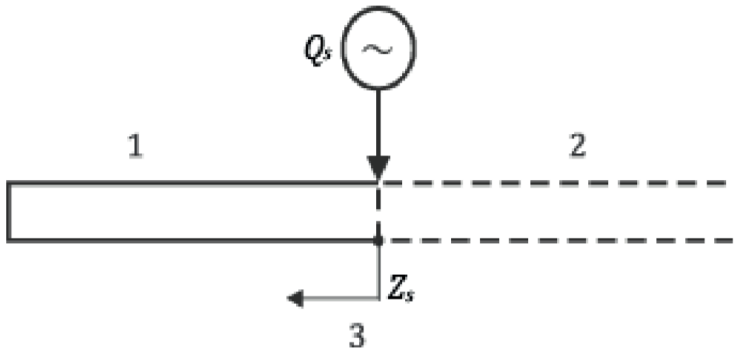

Figure 9 Norton model

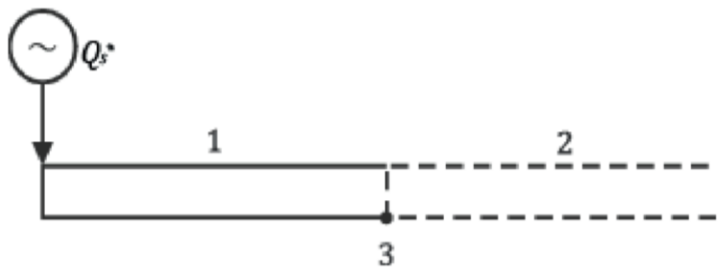

Figure 10 Modified model

1	**Discharge passageway**
2	**Discharge line**
3	**Pump exit**

Table 2 Legend

Initially, the flow ripple at the outlet of the pump can be correlate with the characteristic impedance of the hydraulic circuit Z_C which depends on the unsteady viscous friction ξ, the angular frequency ω, the speed of sound and the geometry of the pipe. Additionally, also the wave propagation coefficient of the reference pipe β must be taken into consideration [7].

$$Z_C = \frac{\rho c \xi(\omega)}{\pi r_O^2} \qquad (26)$$

In this standard, as said before, two tests are performed. The only difference among them is in the way the mean pressure, whose value is kept invariant, is reached. In the first test it is achieved by regulating the first loading valve which is the closest to the discharge line. In the second test, the latter valve is fully opened, while the mean pressure is achieved through the second loading valve.
Once the tests are performed and the data are elaborated by a personal computer, the source flow ripple and the source impedance are evaluated for each harmonic of interest obtaining their amplitude and phase. It is important to underline that only the reference pipe is considered to evaluate both Q_{Si} and Z_{Si} and not all the components of the hydraulic circuit such the loading valves.

$$Q_{Si} = j\frac{1}{Z_C}\frac{P_{0i}P_{1i}' - P_{0i}'P_{1i}}{(P_{0i} - P_{0i}')sin(\beta L_r)} \qquad (28)$$

$$Z_{Si} = jZ_C\frac{(P_{0i} - P_{0i}')sin(\beta L_r)}{P_{1i} - P_{1i}'(P_{0i} - P_{0i}')cos(\beta L_r)} \qquad (29)$$

An additional mathematical algorithm is necessary to evaluate the modified source flow ripple $Q_{Si}*$. It is possible to correlate Q_S and Q_S* through the transfer matrix at the outlet of the pump and an equivalent pipe whose length is a function of the resonant frequency of the source impedance Z_s and the speed of sound:

$$Q_S *= Q_S\, cos(\beta_d L_d) \qquad (30)$$

Where L_d is equal to $\frac{c}{4\, f_r}$, while L_r the length of the reference pipe.

4.2.2 INSTRUMENTATION

As in the previous standard, measurements of static values as shaft rotational speed, pressure, flow rate and temperature of the working fluid are necessary. In this case the accuracy of the instrumentations must satisfy the conditions of table 3:

	Shaft rotational frequency %	Mean flow %	Mean pressure %	Temperature ˚C
2015	±0.5	±2.0	±2.0	± 2.0
1996	±1	±2.5	±2.5	± 2.0

Table 3 Static instrumentation accuracy

Thus, as we can see in this standard the permissible variations during the test are more stringent. Moreover, also the fluid property must follow the accuracy shown in table 4:

	Density %	Viscosity %	Bulk Modulus %
2015	±2.0	±5.0	±5.0
1996	±2.0	±5.0	±5.0

Table 4 Fluid properties accuracy

While for the dynamic measurements, the two pressure transducers used must have in the range of interest of 50 Hz to 4000 Hz the accuracy of table 5:

	Amplitude	Phase	Frequency
2015	± 1%	± 1˚	± 0.5%
1996	± 1%	± 1˚	± 0.5%

Table 5 Dynamic instrumentation accuracy

Which corresponds to the same accuracy of the “secondary source” standard.

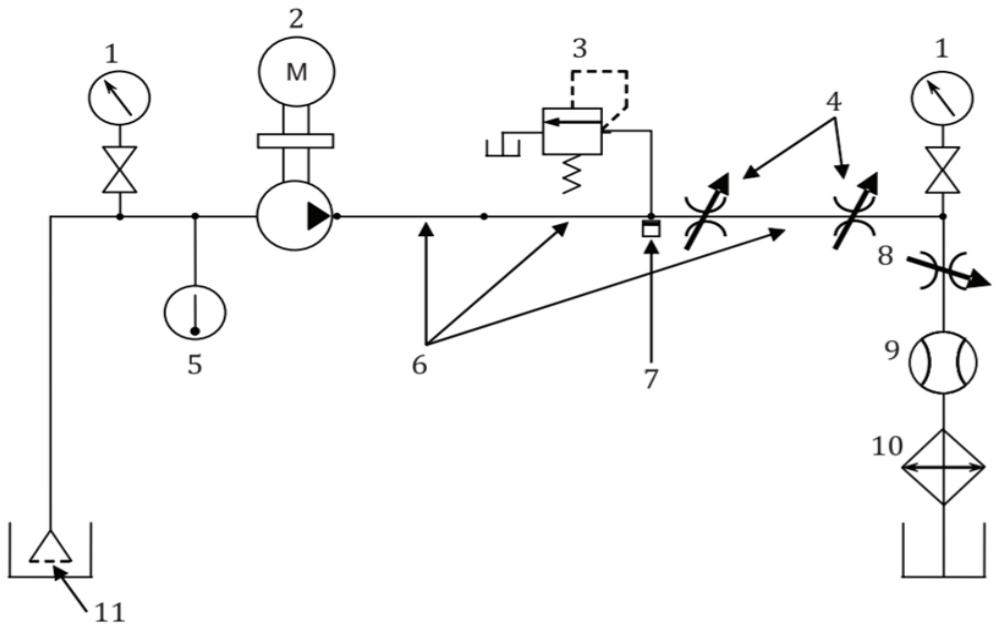

1	Bourdon tube pressure gauge
2	Prime mover
3	Relief valve
4	Loading valves
5	Temperature meter
6	Pipe
7	Piezoresistive pressure transducer
8	Back pressure valve
9	Flow meter
10	Cooler
11	Strainer

Figure 11 Hydraulic circuit

As we can see in Figure 11, the flow meter is installed at the end of the hydraulic circuit, after the second loading valve, while the temperature is measured in the correspondence of the tank. For the mean pressure, a different typology of instrumentation is used between the inlet and the outlet of the pump. To measure the inlet pressure, a pressure gauge of Bourdon tube is used while to measure the mean outlet pressure, a piezoresistive transducer or a strain gauge transducer are used, (the bourdon type is avoided). To measure the fluctuations of pressure, two pressure transducers are positioned one at the inlet and the other at the outlet of the reference pipe. Three different pipes are installed between the outlet port of the pump and the second loading valve. The closest to the pump is the reference pipe whose dimensions are in accordance with the pumping frequency. To obtain data that are not influenced by turbulence effects a pipe whose length is about 200-300 mm is installed between the second pressure transducer and the first loading valve. It is called the connecting pipe. Finally, the extension pipe is installed between the two loading valves. It has the scope of modifying the shape of vibration of system 1 respect to system 2. The dimensions of this pipe are also function of the pumping frequency. Additionally to the loading valves, other two types of valves are installed. A back pressure valve and a pressure relief valve to prevent an excessive outlet pressure.

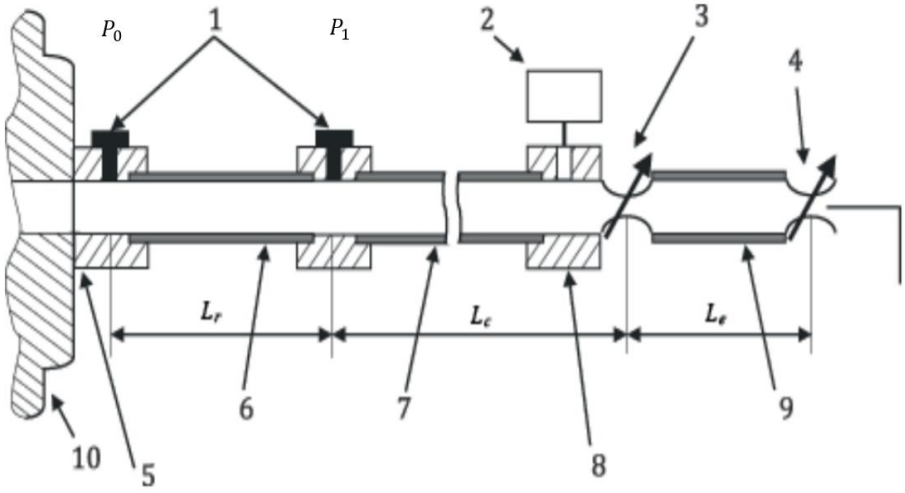

Figure 12 Pipe arrangement

To process the data, several components must be added to the test rig. An amplifier is coupled between the pressure transducers and the analysing recorder. Additionally, a personal computer is necessary to process the data acquired.
During the test, some precautions must be taken. To avoid the presence of air inside the hydraulic circuit, at the beginning of the test, the two loading valves must be opened for a sufficient time frame [7]. Then to start with the first pressure measurements, the first loading valve must be regulated to have the required mean outlet pressure. For the second measurements, a similar path must be followed for the other loading valve. Once $P_0(t)$, $P_1(t)$, $P_0'(t)$ and $P_1'(t)$ are recorded it is possible to calculate all the desired parameters.
Finally, considering an infinite transmission line impedance Z_e, it is possible to compute the amplitude of the blocked acoustic pressure ripple for each harmonic as:

$$|P_{bi}| = |Z_{Si}||Q_{Si}| \qquad (31)$$

Additionally, considering all the ten harmonics taken into consideration, the root mean square of the blocked acoustic pressure is computed as:

$$|P_{bRMS}| = \sqrt{\frac{|P_{b1}|^2 + \ldots + |P_{b10}|^2}{2}} \quad (32)$$

4.3 COMPARISON

It is possible to understand how with the introduction of the 2015 version the ISO has simplified remarkably the test. Firstly, by avoiding the secondary source term, the accuracy of the test increases significantly, because a possible overlap of frequencies between the secondary source and the test pump is prevented.
Moreover, the “two pressures two systems” method makes use only of two pressure transducers to compute the fluctuations of pressure while in the secondary source method three are needed, leading to a decrease in the cost of the instrumentation and in the possibility of a propagation of the errors. In addition, the knowledge of the bulk modulus of the fluid is not yet a problem as well as the computation of the speed of sound.
Furthermore, it is important to state that the easiness of computation of the source impedance and the source flow ripple for the last version of the standard is noticeable respect to the 1996’s one. In fact, if in one standard are needed only the pressure measurements of the two pressure transducers, the characteristic impedance and the geometry values of the reference pipe, in the other, different parameters are requested, especially if the bulk modulus is an unknown variable. In addition, in the 1996 version are also necessary additional mathematical calculations to convert the secondary source frequencies into the test pump’s ones.
Comparing the two test rigs notable differences are present. In the latest version two loading valves are present instead of just one, three different types of pipes constitute the hydraulic circuit while in the other only one is needed. Instead, in the previous version, due to the presence of the secondary source, a ball valve to disconnect the two sections of the circuit is mandatory. On the other hand, since the pressure measurements in system 1 and system 2 must start coherently with the same angular reference, a trigger signal is necessary. Therefore, depending on the response of the digital scope additional errors could be introduced. Additionally, a remarkable difference consists, depending on the knowledge of the bulk modulus, in the use of different methodologies of test in the secondary source method, while in the last version a unique test is performed since the bulk modulus is an entry parameter.
Despite the differences, some common procedures are considered. For example, the pump and the electric motor are coupled in such a way to prevent the additional presence of vibrations while to avoid the presence of air in the hydraulic circuit the loading valve are left fully opened for a certain time before recording the pressure fluctuations.
To sum up, it is important to state that with the introduction of the two pressures two systems test, if in one hand a simplification in the mathematical model is introduced. On the other hand, even if the hydraulic circuit is changed to modify the mode of vibration, the differences found between the two systems are not so relevant. In fact, the values measured by the two pressure transducers are very similar among the first and the second set of measurements. Thus, it is difficult to capture the distinctions especially if high pressure transducers are used. Moreover, respect the standard of the 1996, only ten harmonics are taken into consideration, making difficult a good discretization of the source impedance and the flow ripple source.

CHAPTER 5

TEST BENCH DESIGN

This chapter describes the methodology to design a test bench for the computation of the source flow ripple and the source impedance of positive-displacement pumps. To do so, the standard ISO 10767:1-2015 is followed. To achieve a test bench suitable for a wide range of pumps we have decided to consider three pumps. In the specific two external gear pumps and an axial piston pump. Therefore, three kits are designed. The test bench will be equipped with an electric motor suitable for providing 200kW of power and with a rotational speed up to 2500 rpm. Therefore, the bench test will be suitable to achieve a maximum torque of 765 Nm. In addition, considering a maximum working pressure equal to 300 bar, the theorical volumetric capacity is equal to 160 cc/rev. Moreover, in accordance with the standard ISO, for the external gear pumps the rotational speed is limited to 2000 rpm (maximum pumping frequency achievable equal to 400 Hz).

The test bench can be divided in three sections:

- Mechanical.
- Electrical.
- Software.

5.1 MECHANICAL

The mechanical section of the test bench regards in the specific the hydraulic circuit. It consists of an electric motor, a positive-displacement pump, two piezoelectric pressure transducers, a piezoresistive pressure sensor, a relief valve, two loading valves, three steel pipes and a flow meter. Moreover, to connect the different components is made use of a flange, two mounting blocks and different hydraulic fittings.

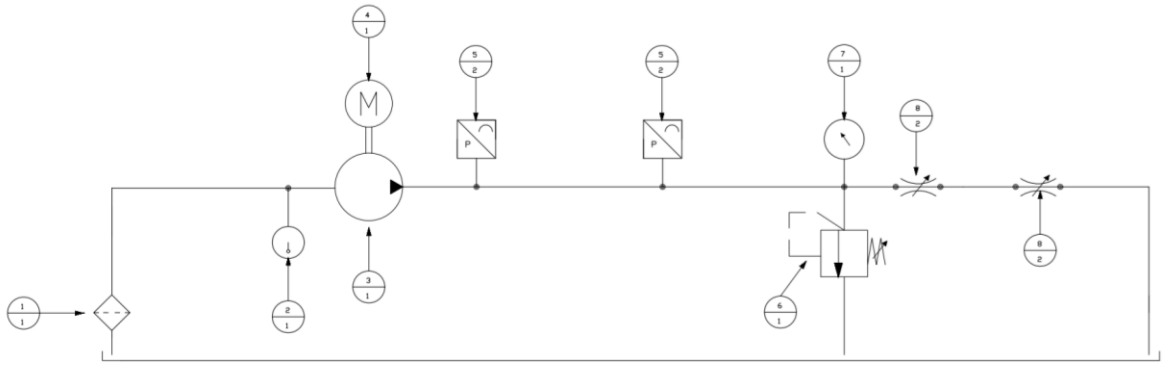

Figure 13 Hydraulic scheme

5.1.1 ELECTRIC MOTOR

During the design of the test bench, we consider an electric motor suitable for providing 200kW of power and with a rotational speed up to 2500 rpm.

5.1.2 POSITIVE-DISPLACEMENT PUMPS

To achieve a test bench suitable for a wide range of positive-displacement pumps we decide to take into account two external gear pumps and an axial piston pump. In the specific:

- Cassapa Polaris PL20-16.
- Cassapa Magnum HD 30-38.
- Lindle HPR 95-02.

They have different dimensions, different working principles and go from a 16.85 cc/rev up to 94.7 cc/rev. In addition, they are distinguished for the type of mounting flange, having respectively a type SAE A, SAE B and a SAE C flange. It is important to remember that these pumps are just an arbitrary choice and that the designed kits are suitable for every positive-displacement pump with similar dimensions.

5.1.3 STEEL PIPES

The differences among the three kits are attributable to the pump outlet port's dimension and to the maximum frequency of interest. As specified in the standard [7], the steel pipes' internal diameter should be between the 80% and the 120% of the pump outlet port. Moreover, their length depends on their position in the hydraulic circuit. At this regard, we distinguish the three steel pipes and call them with different names according to the standard.

- Reference pipe, it connects the pump outlet port with the first mounting block.
- Connecting pipe, it connects the two mounting blocks and has the function of avoiding that the turbulence effect modifies the pressure fluctuation data.
- Extension pipe, it connects the two loading valves and has the function of modifying the vibration mode that occurs in the circuit between system 1 and system 2.

The reference and the extension pipe's lengths depend on the maximum frequency of interest which is the tenth harmonic f_{10} of the pressure ripple. Observing that the pumping frequency is equal to

$$f_p = f_{shaft} \cdot z \qquad (33)$$

where z is the number of pumping elements, and that the tenth harmonic is equal to

$$f_{10} = f_p \cdot 10 \qquad (34)$$

finally, the pipes' length is computed as

$$l = x \cdot (c/2f_{10}) \qquad (35)$$

where x is a value between zero and one and takes into consideration the margin for ill condition. While c is the speed of sound and it is computed following the standard ISO 10767:1-2015 [7]. Its initial value is computed through the fluid's bulk modulus and density as:

$$c_0 = \sqrt{\frac{B}{\rho}} \qquad (36)$$

and finally, its quality is improved by considering the elasticity of the pipe. Consequently, the new speed of sound value is evaluated as

$$c = \sqrt{\frac{1}{\frac{1}{{c_0}^2} + \frac{(D_r + h)\rho}{Eh}}} \quad (37)$$

where D_r is the internal diameter of the pipe while h its thickness.
On the other hand, the connecting pipe's length has a value in the range between 200 mm and 300 mm. In our design we decide to choose the maximum value. Moreover, it is important to state that for the first pipe the length must be considered as the distance between the two piezoelectric sensors. For the connecting pipe as the distance between the second piezoelectric sensor and the second mounting block. Finally for the extension pipe as the distance between the two loading valves.

5.1.4 PIEZORESISTIVE SENSOR

To measure the mean working pressure a piezoresistive transducer is installed at the inlet of the first loading valve. This instrument exploits the piezoresistive effect. Consequently, when a pression is applied to a strain gauge it is deformed and its electrical resistance changes in value and finally an output value, in terms of Volts is generated through a Wheatstone bridge circuit. This type of transducer is very suitable for measuring static pressure because does not present the problem of drift which is a loss in time of the value measured.

5.1.5 PIEZOELECTRIC PRESSURE TRANSDUCER

To measure pressure fluctuations, standard pressure gauge cannot be used because they have a low value of natural frequency leading to incorrect data sampled. Therefore, two piezoelectric pressure transducers are considered during the design of the test bench. One located in the flange and the other in the first mounting block. This type of instrumentation, as it is possible to understand from its name, is composed by a piezoelectric material. The main function of the crystal is to generate an electric charge when a force is applied to itself. This effect is called piezoelectricity and the electrical charge generated is directly proportional to the pressure applied. The charge, then is converted to a voltage signal through a charge amplifier. This device, depending on the working condition, can be installed inside the pressure transducer or externally. Furthermore, piezoelectric transducers cannot be used in case of static pressure because the measurements will be lost in time due to drift.

5.1.6 PRESSURE SENSOS ADAPTERS

The two types of pressure sensors are equipped with a specific adapter. Thus, during the design of the flange and of the two mounting blocks, it is necessary to consider the presence of a nut screw. In both cases it is located in the upper side of the mechanical parts. The piezoelectric and the piezoresistive sensors chosen for the sizing of the nuts screw are respectively the Kistler 601 and the WIKA MH-3. Their adapters have different dimensions and consequently also the two nuts screw. For their sizing, the following dimensions are considered:

- Piezoelectric sensor

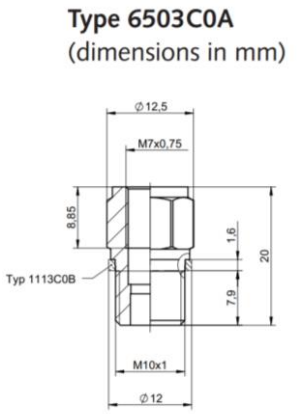

Figure 14 Piezoelectric sensor adapter

The flange and the first mounting block are provided with a M10 nut screw.

- Piezoresistive sensor

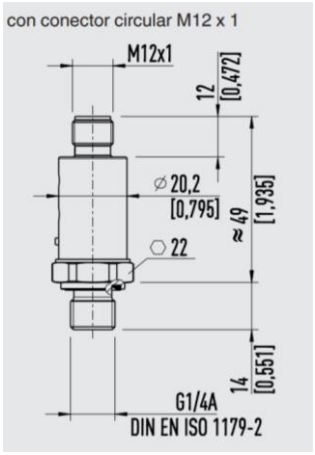

Figure 15 Piezoresistive sensor adapter

The second mounting block is provided with a G ¼ nut screw.
The nut screw's dimensions are the same among the three kits. On the other hand, the dimensions of the flange and the mounting blocks depend on the pipes' size and consequently change among the kits.

5.1.7 OUTLET PORT FLANGE

The flange has the function of connecting the positive-displacement pump with the rest of hydraulic circuit. In addition, here is located the first pressure transducer. The dimensions of the internal and external holes correspond to the ones of the pipes.

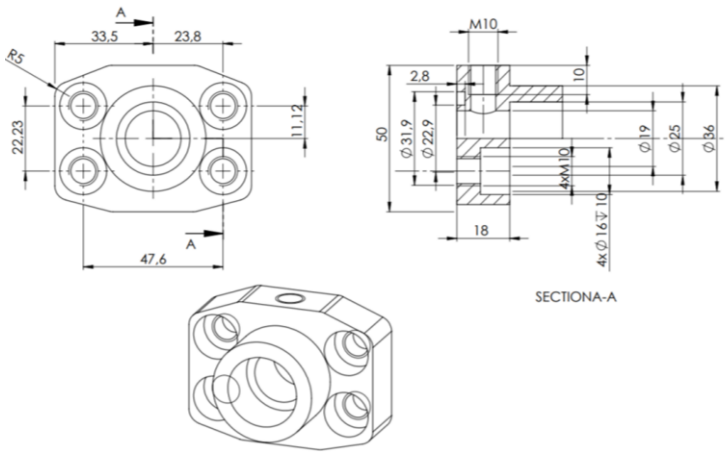

Figure 16 Kit B flange

5.1.8 1st MOUNTING BLOCK

The first mounting block is located between the outlet of the reference pipe and the inlet of the connecting pipe. It is provided with a nut screw suitable for the piezoelectric adapter and with two threaded holes in the rear and the front sides. Their dimensions as well as the internal diameter's ones are in accordance with the pipes' dimensions.

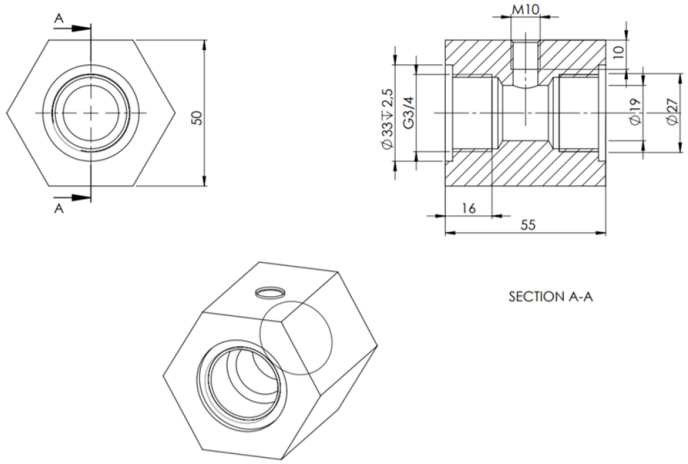

Figure 17 Kit B-1st mounting block

5.1.9 2nd MOUNTING BLOCK

The second mounting block is located between the outlet of the connecting pipe and the first loading valve. It is provided with a nut screw suitable for the piezoresistive adapter and with three threaded holes located in the rear, in the front and in the lateral sides. The lateral port is connected with the relief valve, while the front one with the first loading valve. Their dimensions are in accordance with the two valves while the rear side threaded hole with the pipe dimensions.

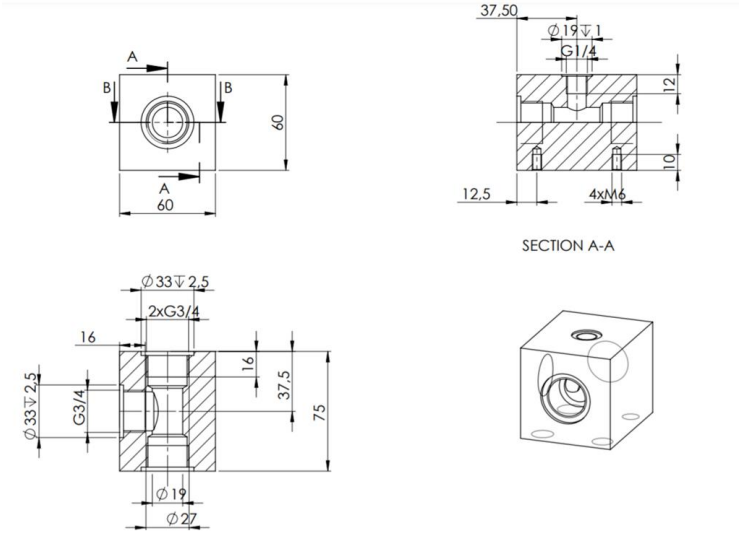

Figure 18 Kit B-2nd mounting block

5.1.10 RELIEF VALVE

To control the maximal pressure in the hydraulic circuit, a pressure relief valve is required. It is located in the second mounting block. For the design purposes we consider the Roquet SGRA06 whose port size is a G ¾ and allows to work up to 350 bar.

5.1.11 LOADING VALVE

To regulate the working pressure two different loading valves are necessary. The first one is located at the end of the connecting pipe, while the second one at the end of the extension pipe. The objective of using two different loading valves is to obtain two different vibration modes in the system 1 and in the system 2. For the design purpose depending on the positive-displacement pump selected, we consider different models of the needle valve Walvoil. The model VRFB9003 for the first kit, the model VRFB9004 for the second kit and finally the model VRFB9005 for the last one. The outlet port dimensions of the loading valves are respectively G ½, G ¾ and G1.

5.1.12 FLOW METER

Finally, a flow meter is mounted and connected to the second loading valve through a steel pipe whose dimensions are arbitrary since the standard does not provide any information.

5.1.13 1st KIT

To design the first kit, we consider the Cassapa Polaris PL20-16, an external gear pump whose main characteristics are listed below:

Volumetric capacity	$\mathbf{16.85\ cc/rev}$
Maximum continuos pressure	$250\ bar$
Maximum velocity	$3500\ rpm$
Mounting flange	$SAE\ A$
Inlet port size	$SAE\ flanged\ code\ MB$
Outlet port size	$SAE\ flanged\ code\ MA$

Number of teeth	12

Table 6 Cassapa Polaris PL20-16's characteristics

Considering that the outlet port is equal to 12.5 mm we chose for the pipes an internal diameter equal to 13 mm and a thickness of 1.5 mm. Additionally, considering a rotational speed equal to 1500 rpm and the number of teeth we found the tenth harmonic equal to 3000 Hz. Therefore, the length of the reference pipe and of the extension pipe is equal to 200 mm. On the other hand, the connecting pipe's length chosen is equal to 300 mm. Considering their sizes, the hydraulic pipes can work with a pressure up to 259 bar.
Coherently with the pipes' dimensions, the flange and the mounting blocks are designed. The flange has an internal hole of 13 mm while the external is equal to 16 mm. In addition, as explained before, it is provided with a lug nut with a M10 threaded hole.
The first mounting block is realized with G ½ port sizes and with an internal hole equal to 13 mm. Moreover, it is realized a lug nut with the same dimension of the previously one.
The second mounting block is provided with G ½ threaded holes in the front and rear side, while with a G ¾ threaded hole in the lateral side.

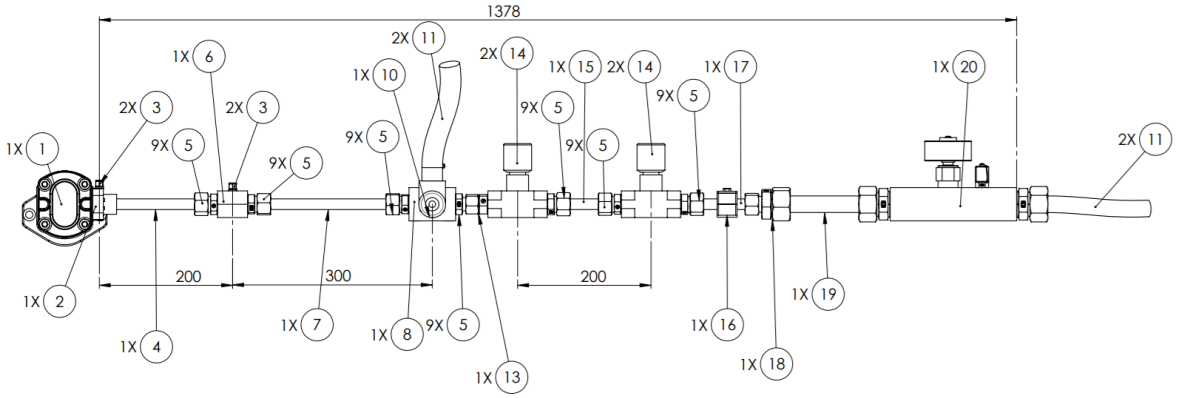

Figure 19 Kit A-Hydraulic circuit

5.1.14 2nd KIT

For the design of the second test kit, we consider the Cassapa Magnum HD 30-38, an external gear pump whose main characteristics are listed below:

Volumetric capacity	$39.27\ cc/rev$
Maximum continuos pressure	$270\ bar$
Maximum velocity	$3000\ rpm$
Mounting flange	$SAE\ B$
Inlet port size	$SAE\ flanged\ code\ MC$
Outlet port size	$SAE\ flanged\ code\ MB$
Number of teeth	12

Table 7 Cassapa Magnum HD 30-38's characteristics

The pump outlet port is equal to 19 mm and the pipes' internal diameters have the same dimension while their thickness are equal to 3 mm. The rotational speed considered is 1500 rpm and considering the 12 teeth we found the tenth harmonic equal to 3000 Hz. Therefore, the length of the reference pipe and the extension pipe is equal to 200 mm. As before, the connecting pipe's length is equal to 300 mm. Taking into account the thickness of the pipes, the maximum working pressure is 330 bar.
The flange connecting the outlet port to the circuit has an internal hole of 19 mm and the external is equal to 25 mm as the values of the pipes. Furthermore, the lug nut has a M10 threaded hole.

The first mounting block is realized with G ¾ port sizes and with an internal hole equal to the pipe's internal diameter. Finally, is realized a lug nut with the same dimension of the previously one.
The second mounting block is provided with G ¾ threaded holes in all the three sides and with an internal hole whose dimension is the same of the first mounting block.

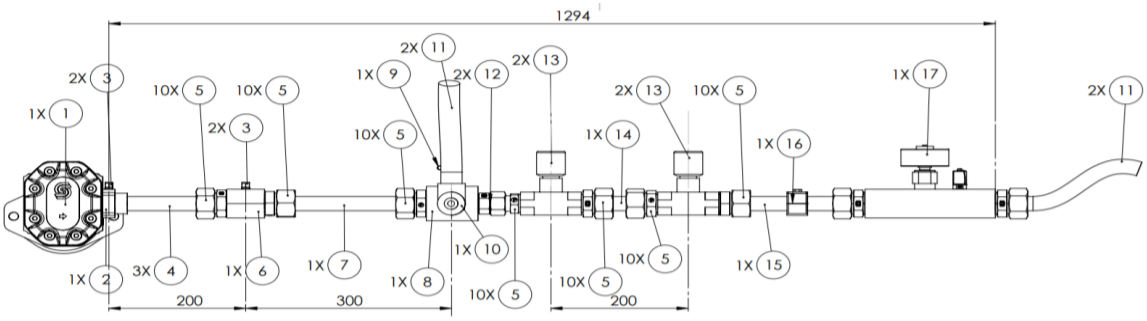

Figure 20 Kit B-Hydraulic circuit

5.1.15 3rd KIT

Finally, for the realization of the last kit, an axial piston pump is chosen. It is the Lindle HPR 95-02 whose main characteristics are listed below:

Volumetric capacity	$\mathbf{94.7\ cc/rev}$
Maximum continuos pressure	$350\ bar$
Maximum velocity	$2500\ rpm$
Mounting flange	$SAE\ C$
Inlet port size	$SAE\ 2"$
Outlet port size	$SAE\ 1"$
Number of pistons	9

Table 8 Lindle HPR 95-02's characteristics

The pump outlet port is equal to 25.4 mm and we chose for the pipes an internal diameter equal to 27 mm and an external equal to 34 mm. Using a rotational speed equal to 1500 rpm and taking into account 9 pistons, the pumping frequency is equal to 225 Hz and so the tenth harmonic equal to 2250 Hz. Therefore, the length of the reference pipe and of the extension pipe is equal to 250 mm. As for the previously tests the connecting pipe has a length equal to 300 mm. Considering the pipe's dimensions, the maximum pressure achievable during the operation is 285 bar.
The flange is designed with an internal hole of 27 mm while the external of 34 mm.
The first mounting block is realized with a G1 port size and with an internal hole equal to 27 mm. For the realization of the lug nut for both the flange and the mounting block the same sizes of the previously cases are selected.
The second mounting block is provided with G1 threaded holes in the front and rear side, while with a G ¾ threaded hole in the lateral side. Its internal hole is equal to 27 mm.

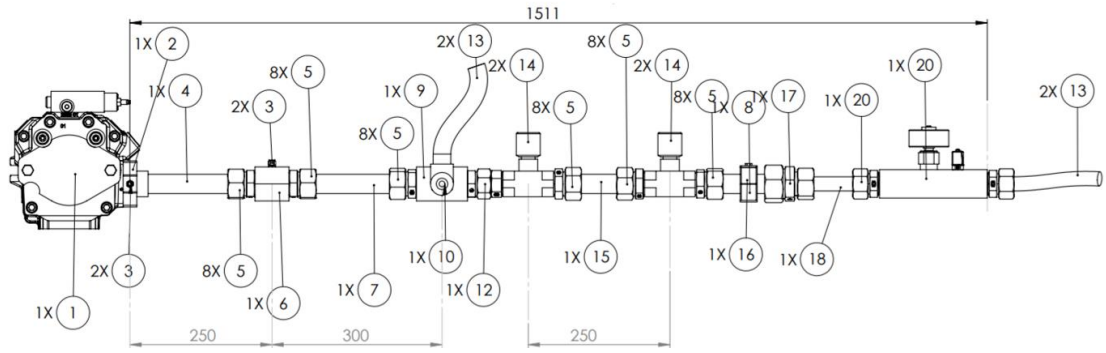

Figure 21 Kit C-Hydraulic circuit

5.2 ELECTRICAL

Considering that the aim of the test is to compute the source flow ripple and the internal impedance of positive-displacement pumps, different electrical components are required.

5.2.1 ANALYSING RECORDER

The standard suggests the use of a 24-bit analysing recorder to sample the pressure fluctuations. In addition, this instrument has the scope of sampling also the mean working pressure. To work properly the recorder should also be connected to an inductive detector. In this way, it is possible to start the sampling of the fluctuations with a coherent reference system and not randomly. In addition, depending on the frequency of interest, the correct sample frequency must be chosen. According to the Nyquist-Shannon theorem it should be at least 2.5 time the tenth harmonic.

5.2.2 CHARGE AMPLIFIER

The analysing recorder to obtain the required signal from the piezoelectric pressure transducer must receive a voltage signal. Therefore, a charge amplifier is required to convert the charge signal.

5.2.3 TRIGGER SIGNAL

As explained in the previous part, a trigger signal is required to perform a correct test. Therefore, an inductive detector should be connected to the electrical motor achieving the dual function of generating a trigger signal and of measuring the rotational speed.

5.2.4 POWER SUPPLIER

Finally, a power supplier should be considered. It has the function of powering the electrical devices.

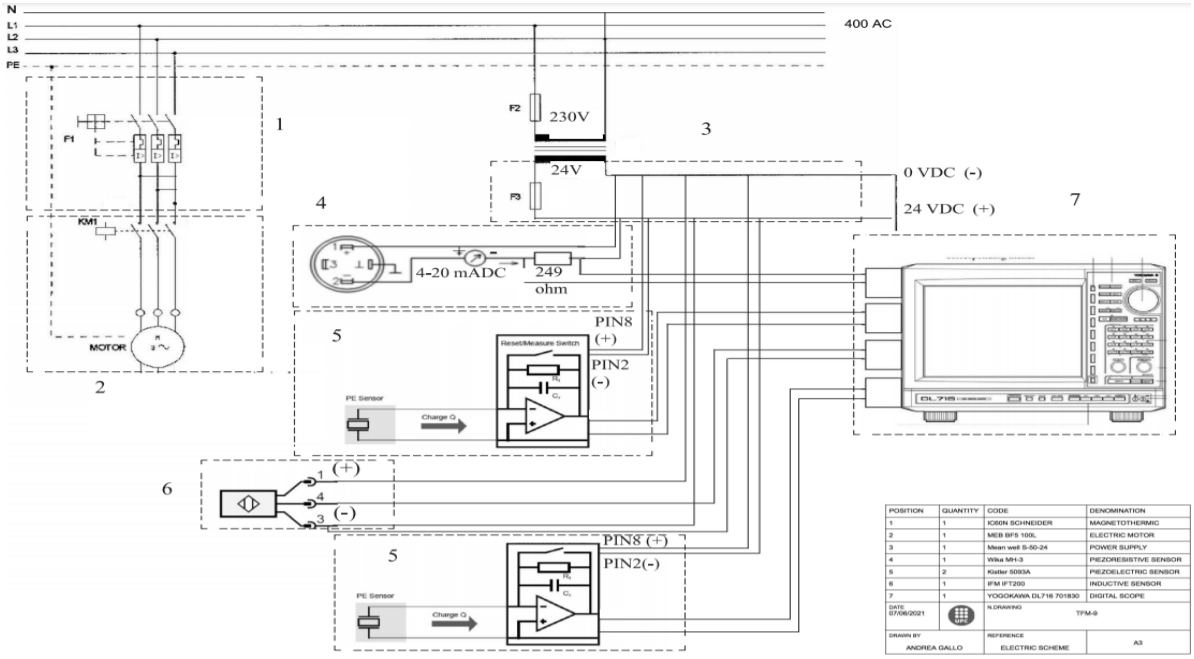

Figure 22 Electric scheme

5.3 SOFTWARE

To process the data obtained through the analysing recorder it is mandatory the use of a personal computer where there are installed software like Excel and Matlab R2020b.

5.3.1 EXCEL

Usually, the majority of recorder gives an Excel sheet as output data. Therefore, a basic knowledge of this software is essential. Considering that to convert the pressure time-signal in the harmonic spectra it is required to compute the DFT, the use of this software is recommended only as a tool to save the data sampled. To compute the source flow ripple and the source impedance it is preferable to use a software like Matlab.

5.3.2 MATLAB

During the computational part, a Matlab code is written. It is used to compute the DFT, to compute the pump's characteristic values and to perform a direct comparison with mathematical models.
Initially, the data saved in the Excel format are converted to the correct language to be used in this software. Later for the four time-signal the DFT is computed. In this way the respective harmonic spectra are obtained. Therefore, it is implemented an algorithm to search the peaks of amplitude in the frequency of interest. At this regard, to improve the accuracy of the calculation, it is decided to avoid directly saving the value of amplitude of the theorical frequencies of interest. It is better for each harmonic to search the peaks of the DFT in a small range that includes the theorical frequency of interest. Later, the impedance of the reference pipe, the wave propagation coefficient and viscous coefficient are computed. In this way it is possible to calculate for each harmonic the source flow ripple and the source impedance. Subsequently, the source flow ripple in the modified model is computed.

Moreover, the representation of flow ripple in the time domain is given. In addition, to give a demonstration of the utility of these characteristic values, the blocked acoustic pressure is calculated. The final part of the code also provides a comparison of the experimental results with the theorical models.
The Matlab code is present in the document “Annexes”.

```
For i=1:10
harmonic=1st harmonic*i;
end
for i=1:10
for k=((harmonic(i)-10):(harmonic(i)+10))
if absolute(dftvector(k)>localmaximum)
save dftvector(k) in pressurevectore
end
end
```

Figure 23 Pseudo code of the search for pressure ripple’s peaks

5.4 SUMMARY TEST BENCH DESIGN

The steps and the instrumentation to compute the source flow ripple and the source impedance of different positive-displacement pumps are very similar. The main differences are found in the design of some parts of the test bench, as seen in the three kits. In addition, depending on the pump’s working condition, different frequencies of interest are achieved. Thus, following the Nyquist-Shannon theorem, different sample frequency can be used.
To sum up, it is important to state that the unique limitation in the working conditions is linked to the fundamental frequency whose value must no overcome 400 Hz.

CHAPTER 6

USED TEST BENCH

This chapter provides a description of the test bench installed in the Laboratory of Fluid Mechanics of the “Universidad Politecnica de Cataluña”. This is a provisional test bench which will be replaced once the designed one will be installed in the UPC University. To perform our test, we follow the Standard ISO 10767-1:2015 which includes a positive displacement pump, an electric motor to drive the pump, different steel tubes, two Bourdon tube pressure gauges, a piezoresistive transducer, two piezoelectric pressure transducers, a back pressure valve, two loading valves, a relief valve, a flow meter, a temperature sensor, a cooler and a strainer. In addition to the hydraulic circuit, different devices are necessary to process the data sampled. For this reason, the standard suggests the use of a 24-bit analysing recorder which is used to record the value of the pressure fluctuations in time domain and a computer to process all the data and to perform the DFT of the signals sampled.

Position	Instrumentation	Brand and type
1	Electric motor	MEB BF5 100L 44
2	Positive displacement pump	Roquet 1L16DE10R
3	Temperature sensor	Elitech TPM10
4	Piezoelectric pressure transducer	Kystler 601
5	Charge amplifier	Kystler 5039A
6	Piezoresistive pressure transducer	Wika MH-3
7	Manometer	Wika 232.30
8	Loading valve	EDI System SU/M/38
9	Pressure relief valve	Roquet SGRA06
10	Steel pipe	Protubsa
11	Flexible hoses	Voss SP 4
12	Detector	IFM IFT200
13	Hydraulic oil	Renoil B10
14	Analysing recorder	Yogokawa DL716
15	Power supply	Mean well S-50-24

Table 9 Test bench's instrumentation

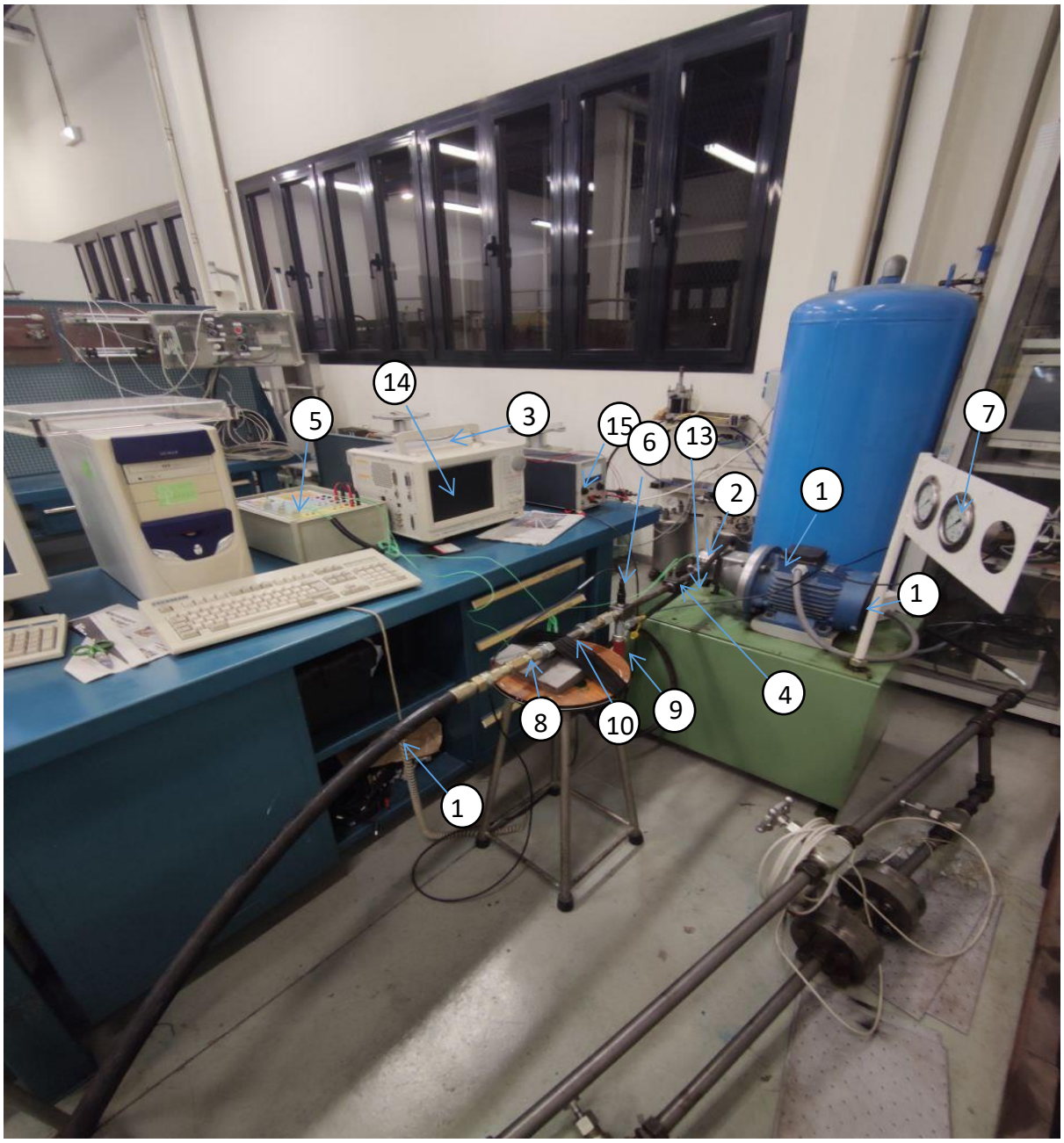

Figure 24 Test bench

6.1 INSTRUMENTATION

The instrumentation used in our test bench finds some differences with the one described in the ISO standard.

6.1.1 MANOMETER

About that, for example of the two Bourdon tube pressure gauges which should be installed respectively at the inlet of the pump and at the outlet of the second loading valve, only one of them is present and is located in the mounting block of the first loading valve. Its purpose is to have a reference value of the mean pressure during the calibration of the two loading valves. Bourdon tubes have a good accuracy and are cheap respect to other pressure sensors, but they are not good in case of vibrations and suffer hysteresis. For this reason, it

is advisable to measure the pump outlet pressure through a piezoresistive transducer. In our test bench, we choose a Wika model 232.30 whose characteristics are listed in the table:

Ambient temperature range	$-40°\ C \div +60°\ C$
Maximum temperature range	$+200°\ C$
Accuracy class	1.6
Ingress protection	$IP\ 65$
Pressure element	$C\ type$

Table 10 Manometer's characteristics

6.1.2 PIEZORESISTIVE PRESSURE TRANSDUCER

To measure the working pressure a piezoresistive transducer is installed at the inlet of the first loading valve. In our test bench the piezoresistive transducer chosen is the WIKA OEM model MH-3. Its current signal lies in the range between 4 and 20 mA and it is converted in tension thanks to a resistance of 249 ohm. Moreover, the transducer is powered at 24 V. This type of transducer is very suitable for measuring static pressure because it does not present the problem of drift which is a loss in time of the value measured. Furthermore, they have good accuracy and do not lose their property with the use. The piezoresistive transducer's main characteristics are shown in table 11.

Ambient temperature range	$-40°\ C \div +100°\ C$
Maximum temperature range	$+125°\ C$
Accuracy	$< \pm 1\%$
Non-linearity	$\pm 0.25\%$
Response time	$\leq 2\ ms$
Long term stability	$\leq \pm 0.2\%$
Vibration resistance	$20\ g$
Shock resistance	$500\ g$
Type of protection	$IP67$
Output signal	$4 \div 20\ mA$
Power supply	$24\ V$

Table 11 Piezoresistive pressure transducer's characteristics

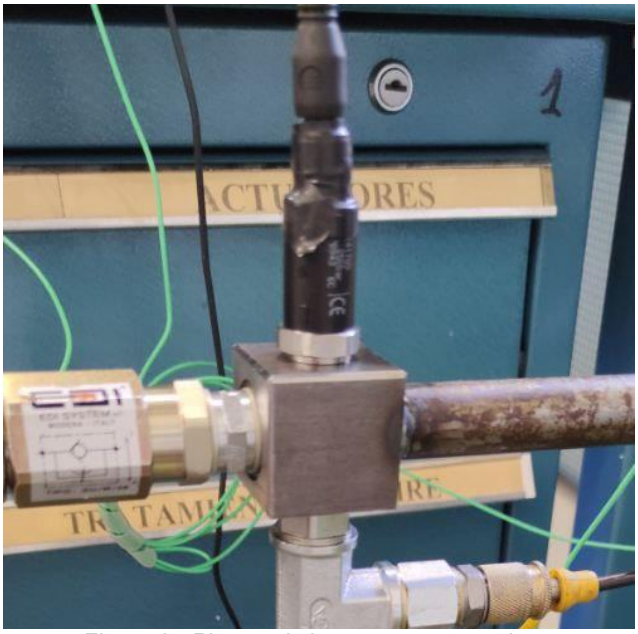

Figure 25 Piezoresistive pressure transducer

6.1.3 PIEZOELECTRIC PRESSURE TRANSDUCER

To measure pressure fluctuations, we install two piezoelectric pressure transducers, the 601 type Kistler high pressure sensors. These types of sensors are equipped with an external amplifier, the Kistler miniature charge amplifier type 5039A. It will be set in the measuring range type II for working between 500 pC and 5000 pC. Its maximum voltage output signal is equal to ± 10 V, which for our tests is a value quite high to overcome. The charge amplifier, furthermore, thanks to its rugged and shock-proof construction is suitable also for industrial application and consequently it is reliable for ours tests. Furthermore, piezoelectric transducers cannot be used in case of static pressure because the measurements will be lost in time due to drift. The Kistler 601's main characteristics are listed below:

Pressure range	$0\ bar \div 250\ bar$
Overload	$500\ bar$
Operating temperature range	$-196°\ C \div +200°\ C$
Sensitivity	$-16\ pC$
Natural frequency	$150\ kHz$
Drift	$\pm 0.5\ pC$
Linearity	$< \pm 0.5$
Capacitance	$5\ pF$
Connector	$M4x0.35$

Table 12 Pressure transducer's characteristics

Furthermore, before the use of both the piezoresistive and the piezoelectric pressure transducers a correct calibration is mandatory.

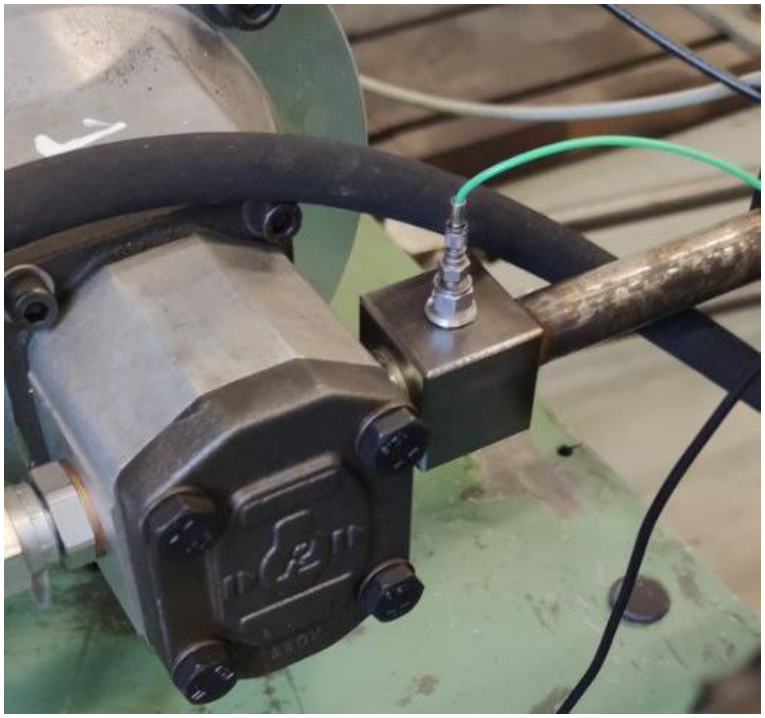

Figure 26 1st Piezoelectric pressure transducer

6.1.4 PRESSURE RELIEF VALVE

To control the maximal pressure in the hydraulic circuit, a pressure relief valve is installed at the inlet of the first loading valve. The valve chosen is the Roquet SGRA06 which is suitable to work with a maximum pressure of 350 bar, in a range of temperature between -20° C and +80° C and with hydraulic oils whose viscosity range is between 32 mm/s^2 and 46 mm/s^2. During the tests, its value is adjusted so that is possible to work with a pressure of over 100 bar without that it enters in actions modifying the vibration mode.

Temperature range	$-20°\ C \div +800°\ C$
Pressure range	$85\ bar \div 175\ bar$
Maximum pressure	$350\ bar$
Oil viscosity range	$VG32 - VG46$
Flow rate	$100\ l/min$

Table 13 Pressure relief valve's characteristics

Figure 27 Pressure relief valve

6.1.5 LOADING VALVES

To regulate the working pressure of ours test, two different loading valves are mounted. The first one is installed at the end of the connecting pipe, while the second one is located at the end of the extension pipe. Both the valves before starting the tests are left opened to let the air out of the hydraulic system. Furthermore, during the tests when the system 1 is employed, the second loading valve must be let fully opened. Similarly, when the system 2 is used, the first loading valve must be let fully opened so that any alteration of the pressure sampling is avoided. The two loading valves are two check flow valve adjustable flow regulator of EDI System model SU/M/38.

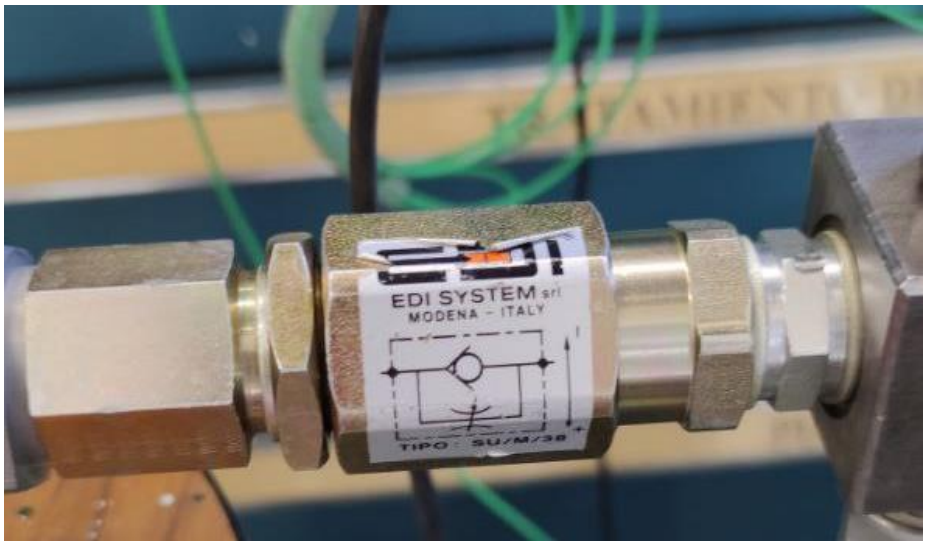

Figure 28 Loading valve

6.1.6 PIPES AND HYDRAULIC FITTINGS

The pump outlet port and the main test rig are connected by a steel pipe whose dimensions are computed depending on the port diameter and the maximum frequency of interest. Considering that the outlet port diameter of our pump is equal to 19 mm and that the standard suggests a steel pipe whose internal diameter should have dimensions in the range of $0.8 < d_{port} < 1.2$, we choose a steel pipe with an internal diameter equal to 16 mm and with the outlet diameter equal to 22 mm. Moreover, considering that the maximum frequency of interest is the tenth harmonic f_{10} of the pressure ripple and that the pumping frequency is equal to

$$f_p = f_{shaft} \cdot Z \qquad (38)$$

where Z is the number of pumping elements that for our pump are equal to twelve and that $f_{10} = f_p \cdot 10$, we compute the pipe length as:

$$l = x \cdot (c/2f_{10}) \qquad (39)$$

where x stands for a value between zero and one, which takes into consideration the margin for ill condition. In our computation we employ a value similar to the one used in the standard, 70%. The second term represents half the wavelength at the maximum frequency f_{max}. Taking into consideration the operating condition of the electric motor, the number of pumping elements, the fluid bulk modulus, its density, the pipe's Young modulus, its dimensions and the margin factor, we find a length value equal to 150 mm for the first part of the pipe which is called the reference one. The second part of the pipe is called the connecting pipe and its function is to avoid that the turbulence effect changes the values obtained. Its length should be within 200 mm and 300 mm and we choose a value equal to 250 mm. Both the internal and the external diameters of the two parts of the pipe have the same values. The reference and the connecting pipe are a unique pipe and three fittings divide the two pipes. In the first two fittings are located the adapters for the pressure sensors and in the last one are located the pressure relief valve, the bourdon pressure tube and the first loading valve.

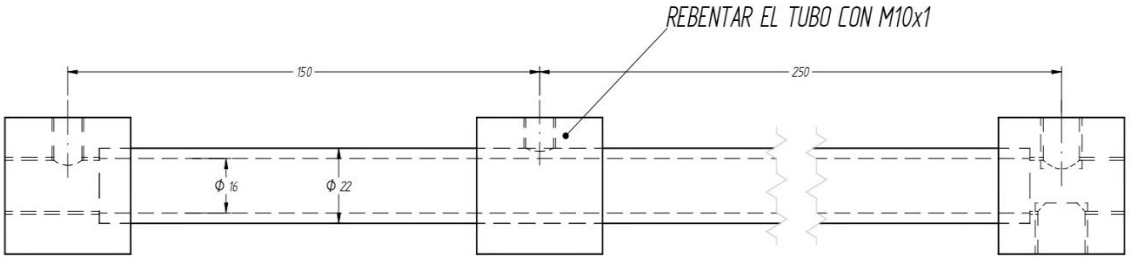

Figure 29 Drawing of the reference and connecting pipes

Moreover, a second steel pipe, that is called the extension pipe, is installed between the two loading valves at which is connected through hydraulic fittings. The aim of this pipe is to change the vibration mode between system 1 and 2. Its dimensions are the same of the reference pipe thus its length is equal to 150 mm with an internal diameter equal to 16 mm and a thickness of 3 mm.
Finally, different flexible hoses are installed. One is located between the second loading valve and the flow meter. Another one connects the relief valve with the tank and another one connects the outlet port of the flow meter with the tank.

Temperature range	$-40°\ C \div +100°\ C$
Maximum pressure	$350\ bar$

Table 14 Flexible hoses' characteristics

6.1.7 HYDRAULIC OIL

For our test, according to the standard DIN 51524-24 LP and ISO 6743/4, the Renoil B10 hydraulic oil is used whose main characteristics are summed up in the following table:

Density at 15° C	876 kg/m^3
Kinematic viscosity at 40° C	32 mm/s^2
Kinematic viscosity at 100° C	5.5 mm/s^2
Viscosity index	>95
Inflammation point	>180

Table 15 Hydraulic oil characteristic

Considering that in ours tests different temperature are achieved, the different kinematic viscosities are listed in the following table:

Working temperature	**Kinematic viscosity**
25° C	68.24 mm/s^2
35° C	39.79 mm/s^2
45° C	30.69 mm/s^2

Table 16 Kinematic viscosity at working temperatures

This type of hydraulic oil meets the requirements of the HLPD hydraulic oils.

6.1.8 TEMPERATURE SENSOR

To evaluate the working temperature, a sensor is installed and located in the tank of the test bench. The computation of the temperature is important since the kinematic viscosity

depends on the temperature as it is possible to see from the following viscosity-temperature diagram

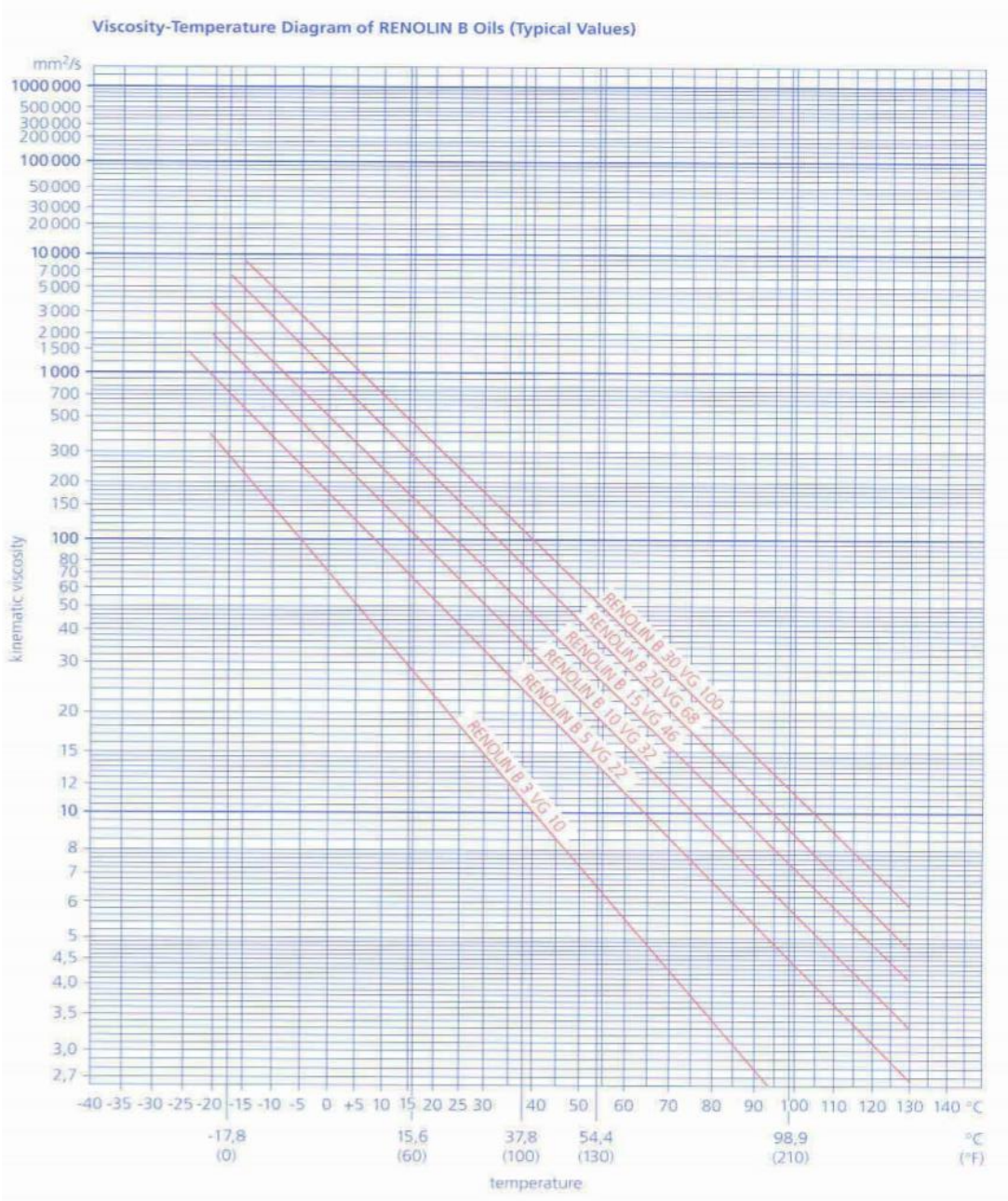

Figure 30 Temperature-viscosity diagram Renoil B10

The digital thermometer used in our test bench is the ELITECH TPM10. Its characteristics are listed below:

Temperature range	$-40° C \div +100° C$
Accuracy	$\pm 1° C$
Resolution	$0.1° C$

Table 17 Temperature sensore's characteristics

6.1.9 TRIGGER SIGNAL

An important consideration to make is the use of a trigger signal. In this way, it is possible to avoid a random starting time for the pressure measurements which would lead to wrong

results. Thus, it is necessary to start the measurements coherently according to a fixed reference. In our test, to obtain a reference pulse signal, a screw is fixed in one fan blade of the electric motor using an industrial glue as it is possible to see from figure 31.

Figure 31 Inductive sensor

In this way, an inductive detector, at each rotation of the fan, can generate a reference signal. The detector chosen is the IFM IFT200 whose characteristics are the following ones:

Switching frequency	$800\ Hz$
Detection range	$7\ mm$
Thread	$M12\ x\ 1$
Temperature range	$0°\ C \div 100°\ C$
Protection class	$IP\ 68$
Supply voltage	$10\ V \div 36\ V$

Table 18 Inductive detector's characteristics

6.1.10 EXTERNAL GEAR PUMP

The positive displacement pump chosen in our study is a Roquet external gear pump 1L16DE10R, whose volumetric capacity is equal to 10.6 cc/r. It is actioned at 1450 rpm, obtaining a mean flow rate of 15 lpm.

Rotation sense	$clockwise$
Driving shaft form	$type\ E$
Port connection	$type\ R$
Max. cont. pressure	$275\ bar$
Max. rpm	$3500\ rpm$
Number of pumping elements	12

Table 19 External gear pump's characteristics

6.1.11 ELECTRIC MOTOR

The triphasic electric motor chosen is the BF 5 100 L, which is actioned at 230 V and 50 Hz with a rotational speed of 1450 rpm.

6.1.12 DIFFERENCE AMONG THE STANDARD AND OUR TEST BENCH

Usually, a cooler is present in a hydraulic circuit because is function is important since the oil viscosity strongly depends on the temperature, (it decreases increasing the temperature). Therefore, if high temperatures are achieved some components of our test bench could not work in a proper way leading to problems in the entire circuit. Considering that the maximum pressure achieved during our tests is equal to 90 bar and that the maximum temperature after two hours of tests is equal to 45° C, a cooler is not installed. Additionally, the standard suggests the use of a strainer which has the function of avoiding the presence of contaminants at the suction of the pump and so a possible damage of the hydraulic machine. It is important to state also that the presence of a strainer can lead to a drop of the inlet pressure and consequently to the phenomenon of cavitation. For this reason, it is necessary to analyze the working conditions to understand if the presence of a filter is mandatory or it is preferable to avoid it. In our case the strainer is avoided due to the possibility of cavitation. Furthermore, to reduce any possibility of occurrence of cavitation, before the tests, the tank was filled further with hydraulic oil. By doing so, taking into account that increasing the level of oil and consequently by decreasing the elevation of the suction port respect to the tank, the inlet pressure is increased.

$$p_{inlet} = p_{atm} - \frac{1}{2}\rho v^2 - g\rho z - \Delta p_{inlet-tank} \qquad (40)$$

Figure 32 Filling the hydraulic oil in the tank

About cavitation, the standard suggests the use of a back pressure valve, which has the double function of avoiding both a drop of pressure and cavitation at the loading valve orifice. In our test bench no back pressure valves are installed, since the possibility of a pressure drop is unlikely due to the presence of a flow meter having a considerable length.

6.1.13 16-BIT ANALYSING RECORDER

The most important difference respect to the ISO standard is the use of a 16-bit analysing recorder respect to a 24-bit type. By doing this, the quality of the signal converted from analogic to digital is reduced. For ours tests is used the Yogokawa DL716-701830 digital scope, whose aims are to sample the pressure fluctuations, the static pressure and to receive a reference pulse signal from the inductive detector.
Moreover, since the pressure data are saved in a floppy disk due to its size limitation, only block sizes equal to 10020 samples can be recorded. Consequently, a lower frequency resolution than the one hoped is achieved, influencing negatively our results.

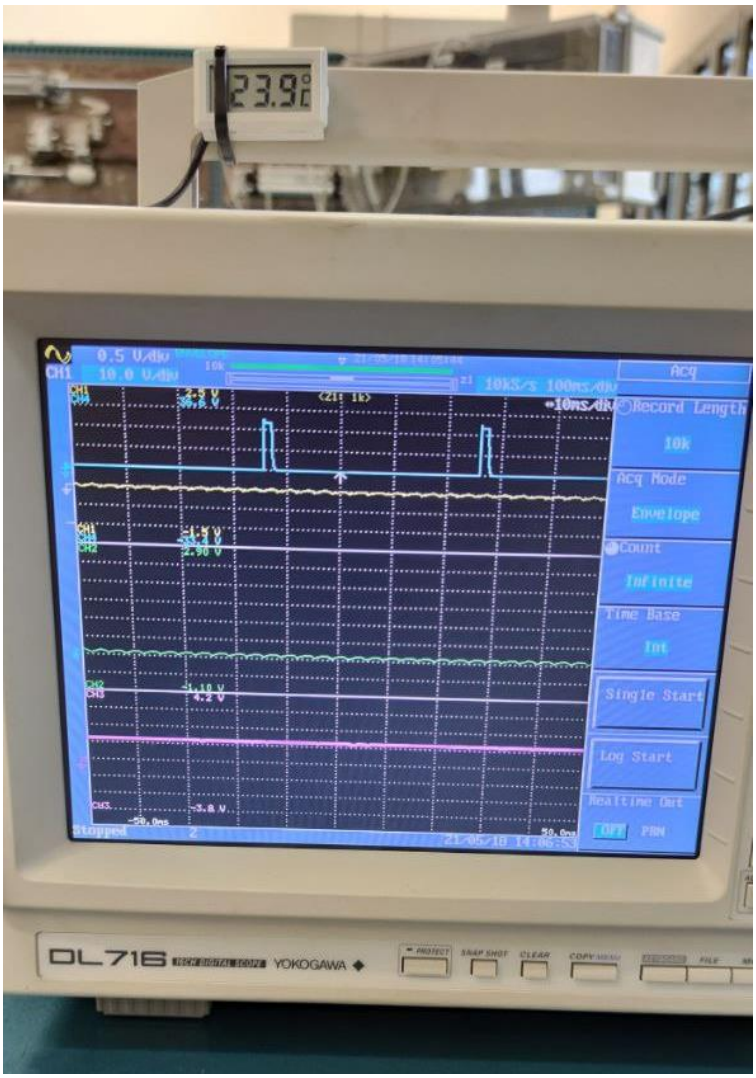

Figure 33 Yokogawa DL716 701830 digital scope

6.1.14 EXCEL AND MATLAB SOFTWARE

To process the data obtained through the 16-bit digital scope, it is mandatory the use of a personal computer where there are installed the software Excel and Matlab. In fact, the data from the DL716 are recorded as an Excel sheet which once saved are processed through a Matlab code. By using the latter software, a discrete Fourier transformation DFT is computed for each pressure ripple signal obtaining the harmonic spectra.

CHAPTER 7

TEST PROCEDURE AND RESULTS

Different tests are performed to characterize the 10.6 cc/rev positive displacement pump and the hydraulic circuit. At this regard, the tests are carried out using three different working pressure, 50,75 and 90 bar. In this way, a direct proof of the Matlab code and the methodology is furnished. Considering that the laboratory of fluid mechanics of the university is used for different experimental procedures, the tests are carried out in various days and at different hours of the day so that it is possible to understand if the results obtained can be influenced by external factors or are coherent among them.

7.1 TEST DESCRIPTION

In every test carried out the procedures followed are the same. Initially, the electronic devices, such as the digital scope, the 24 V power supply and the personal computer are turned on as well as the group electric motor-hydraulic pump while both the loading valve are fully opened.
Later, through the regulation of the first loading valve and the help of the manometer, the desired mean working pressure is set and subsequently the two pressure fluctuations $p0(t)$ and $p1(t)$ of system 1 are recorded at the same time with the digital scope. Considering that the shaft rotational speed of the electric motor is equal to 1450 rpm and that our hydraulic pump has 12 pumping elements (number of teeth), the 10th harmonic is expected to be at 2900 Hz. Consequently, in accordance with the Nyquist–Shannon theorem, the sample frequency f_s chosen in the digital scope is equal to 10 kHz so that our signal can give information up to 5 kHz, (we follow the rule of thumb for which $f_s > 2.5 f_{10}$) . Additionally, due to the memory limitation of the floppy disk, the block size N chosen is equal to 10020 samples obtaining thus, a frequency resolution equal to 0.998 Hz $\left(\frac{f_s}{N}\right)$.
Moreover, as suggested by the standard, during the sampling of the data, the acquisition mode chosen is the envelope one. In this way, the 16-bit recorder is able to avoid the phenomenon of aliasing.
After the first sampling, the first loading valve is fully opened and the second one is regulated to achieve the previous mean pressure. Consequently, the two pressure fluctuations $p0'(t)$ and $p1'(t)$ of system 2 are recorded and saved in the floppy disk as well as for the first system. It is important to remember that both the measurements of system 1 and system 2 are triggered by a square wave signal as explained in chapter 5, so that they start in the same shaft reference point and not randomly.
The data are saved in an Excel format. Thus, to obtain the representation in the frequency domain through the DFT and to compute the main characteristic values of the pump, a Matlab code is required. Firstly, the Excel data are converted into a Matlab format so that it is possible to evaluate the wave propagation coefficient β of the pipe, the unsteady viscous friction effect coefficient ξ, and the characteristic impedance Z_C of the reference pipe. Subsequently, it is possible to compute for each harmonic the source flow ripple $Q_{s,i}$ and the source impedance $Z_{s,i}$, as explained in chapter 4.
Furthermore, it is possible to compute the source flow ripple in the modified model Q_S^*, where the flow fluctuation source is described to be in the inner part of the outlet line of the pump. Thus, the flow ripple is computed as:

$$Q_{S,i}^{*} = \frac{Z_{S,i}}{\sqrt{Z_{S,i}^{2} - Z_{C}^{2}}} Q_{S,i} \qquad (41)$$

Additionally, it is useful to evaluate the time history of the waveform by using the source flow ripple in the modified model instead of the Norton one. Consequently, it is computed as

$$q(t)^{*} = \sum_{i=1}^{10} \left| Q_{S,i}^{*} \right| \cos\left(2\pi f_i t + \psi_i\right) \qquad (42)$$

where ψ_i stands for the phase of the modified flow ripple source.
Finally, for each of the ten harmonics, it is interesting considering a hydraulic model where the impedance Ze at the entrance of the transmission line tends to infinite. Thus, considering a model where the outlet port of the pump is blocked. In such a way, it is possible to compute the blocked acoustic pressure ripple. In fact, if we consider the pressure fluctuation at outlet port of the pump computed through the Norton model

$$P_0 = \frac{Z_s Z_e}{Z_s + Z_e} Q_s \qquad (43)$$

with an infinite value of Z_e, the pressure ripple at the outlet port is equal to the blocked acoustic pressure fluctuations which finally is computed as:

$$\left| P_{b,i} \right| = \left| Z_{s,i} \right| \cdot \left| Q_{s,i} \right| \qquad (44)$$

and additionally, its overall RMS value is computed as:

$$\left| P_{bRMS} \right| = \sqrt{\frac{\left| P_{b,1} \right|^2 + \left| P_{b,2} \right|^2 + \cdots + \left| P_{b,10} \right|^2}{2}} \qquad (45)$$

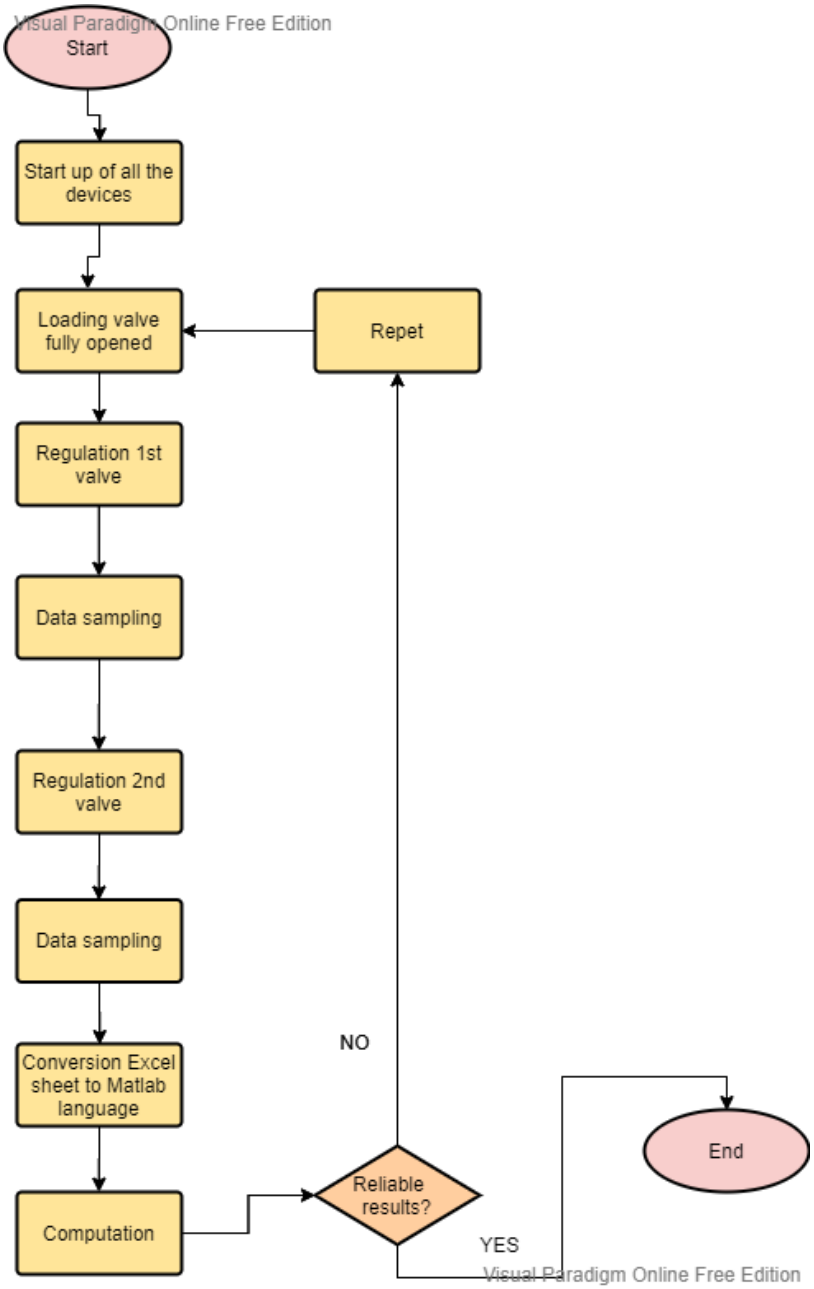

Figure 34 Test procedures flow chart

7.2 TEST VALIDATION METHODS

To understand if the calculation followed to obtain the characteristic values of the pump are reliable three paths can be followed. The first one regards the computation of the source impedance following the lumped and the distributed parameter models described in the ISO Standard 10767:1-1996 [8]. The difference between the two models consists in which factors influence the characteristic values of the hydraulic circuit. In the lumped model, the source impedance is only function of time while in the distributed model it is also function of the space. A rule of thumb to choose the first or the second model is to compare the length of the circuit with the source wavelength. In case of an outlet pathway whose dimension are higher than a quarter of the wavelength, the model to be chosen is the distributed. It consists in studying the discharge passageway as a closed-end length pipe. While in the case that it is possible to use the lumped, the discharge passageway can be described as a single point.

7.2.1 LUMPED PARAMETER

When the lumped system is used, the source impedance is obtained through the equation:

$$Z_{Slumped,i} = \frac{c_1}{(j \cdot f_i)} \quad (46)$$

where $j = \sqrt{-1}$, f_i is the frequency of the general ith harmonic and the coefficient c_1 is computed as

$$c_1 = \frac{1}{n}\sum_{i=1}^{n} Im(Z_{S,i} f_i) \quad (47)$$

7.2.2 DISTRIBUTED PARAMETER

In the case of distributed parameter, the dimension of the pipe's outlet pathway is comparable with the wavelength of the signal and the source impedance of the pump is computed as:

$$Z_{Sdistributed,i} = \frac{c_1}{j \cdot \tan(c_2 \cdot f_i)} \quad (48)$$

with the factors c_1 and c_2 computed through an iterative process.

7.2.3 PRESSURE MODELLING

Furthermore, as suggested in the article "Measurement of flow ripple in positive displacement pumps (effect of approximation model of discharge passage in pump)" written by Choi, Lee and Ji [9], it is possible to compute the relative error between the pressure fluctuations sampled through the digital scope and the ones computed through the characteristic values of the pump. Consequently, using the Norton model and taking into account the continuity of the flow rate, the flow fluctuation at the outlet of the pump, and thus, at the position $x = 0$, is computed as:

$$Q_0 = Q_S - \frac{P_0}{Z_S} \quad (49)$$

While in a generic x position of the hydraulic circuit the pressure fluctuation is computed as:

$$P_x = \cos(\beta l) \cdot P_0 - jZ_C \cdot \sin(\beta l) \cdot Q_0 \quad (50)$$

And finally, using the pressure sampled with the first pressure transducer P_0 it is possible to compute the relative error for the pressure ripple located at the position of the second pressure transducer:

$$relative\ error: \frac{|P_1 - P_{1,model}|}{|P_1|} \quad (51)$$

In this way, the quality of the source flow ripple, the internal impedance and the characteristic impedance are evaluated.

7.2.4 FLOW RIPPLE MODELING

Finally, a useful tool to understand the consistence of the results is modeling the flow fluctuations in time. Consequently, we follow the same approach of chapter 2 where the flow ripple for our type of positive displacement pump is computed as:

$$Q(\psi) = Q_{max} - K\psi^2 \qquad (52)$$

Where considering involute gears and the following constructive parameters

b (tooth width)	**18 mm**
z (number of teeth)	12
r (primitive radius)	15 mm
θ (pressure angle)	20°
ϑ (angular velocity)	1450 rpm

Table 20 Pump's constructive parameters

the factor $K = b\vartheta r^2 cos^2\theta$ is computed.
Furthermore, knowing that the maximum flow rate is equal to 16 lpm, the mathematical model is evaluated and compared with the experimental one.

7.3.1 RESULTS AT 50 BAR

The first test is carried out at a mean pressure of 50 bar and at a temperature equal to 25° C. As it is possible to see from the following figures, the pressure fluctuations in the frequency domain between the system 1 and the system 2 change in values, making clear how the use of the extension pipe modifies the vibration mode of the working fluid. The maximum pressure difference in system 1 is equal to 4.2 bar and it is measured in the first transducer. In the system 2 it is equal to 3 bar and belongs to the second pressure transducer.

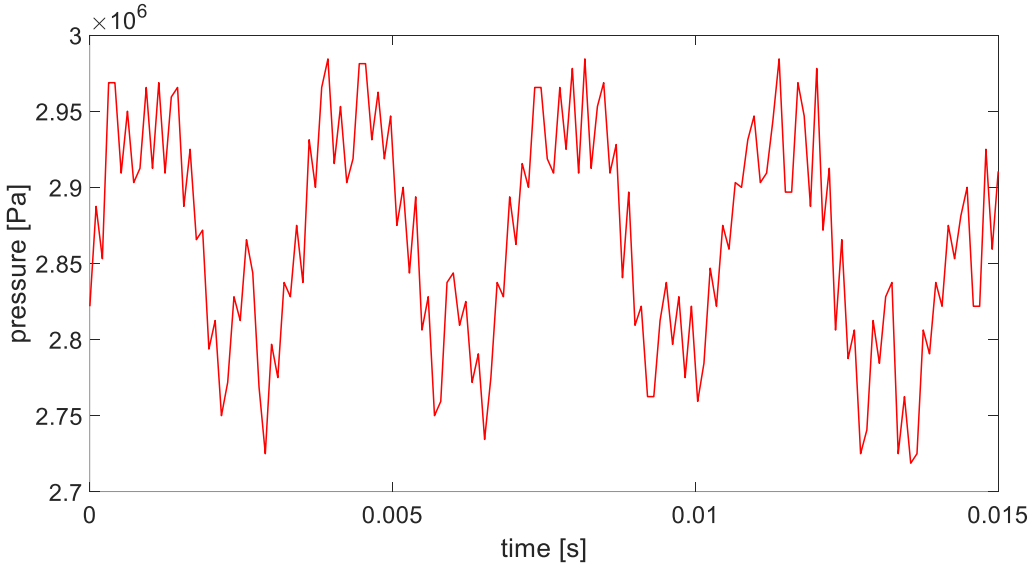

Figure 35 Pressure fluctuations in time

In the harmonic spectra the maximum peaks are located both in the second pressure transducer and at the fundamental harmonic and are equal to 0.82 bar and 0.66 bar for the system 1 and system 2 respectively.

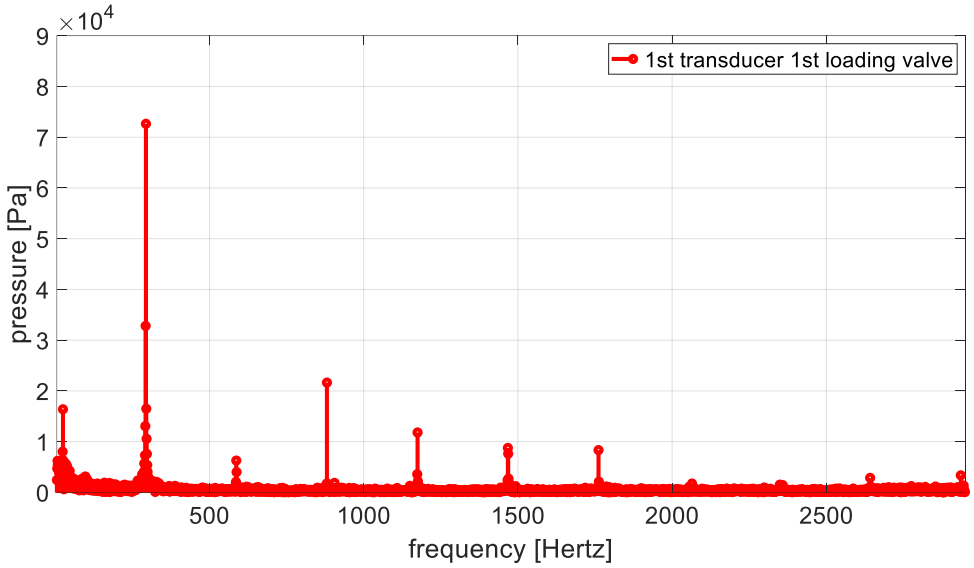

Figure 36 Transducer 1, system 1

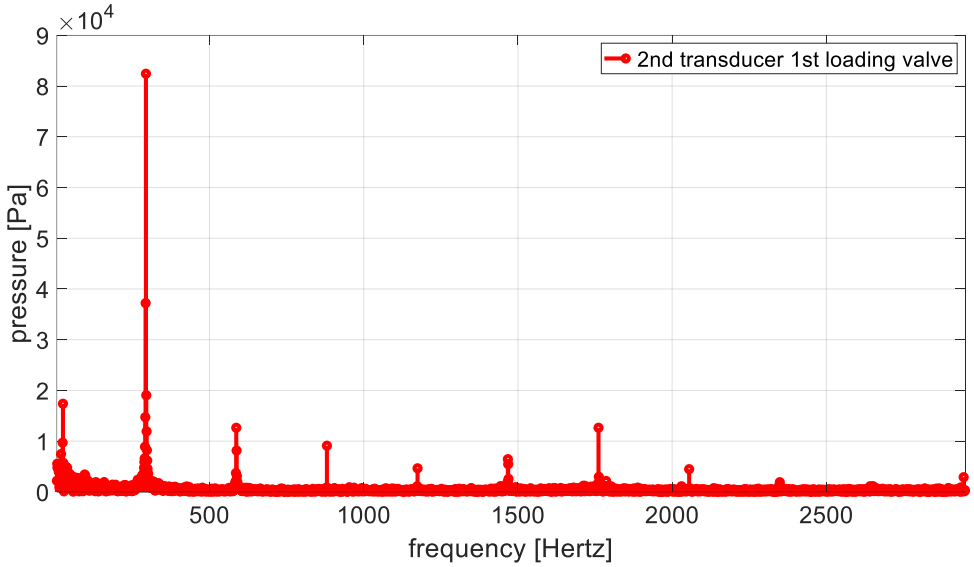

Figure 37 Transducer 2, system 1

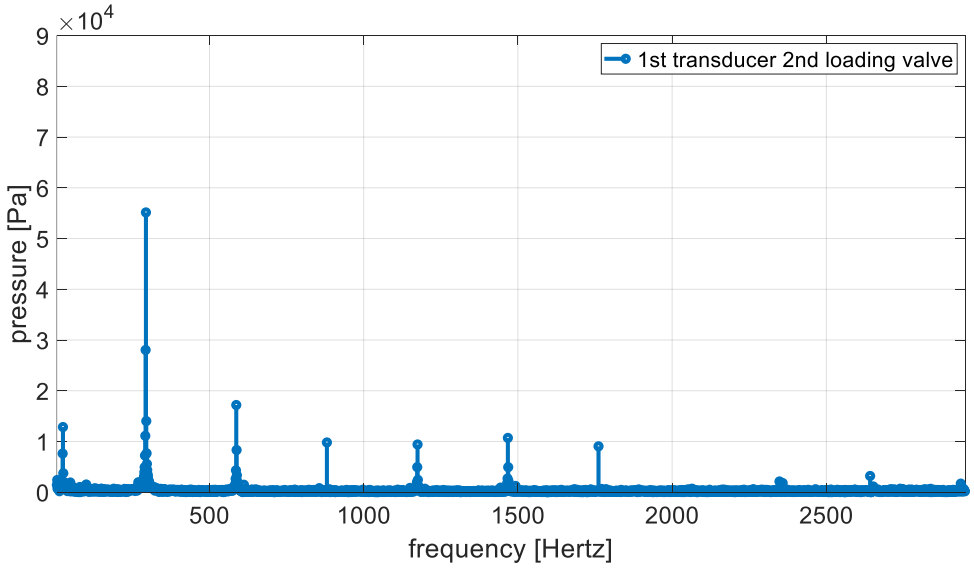

Figure 38 Transducer 2, system 1

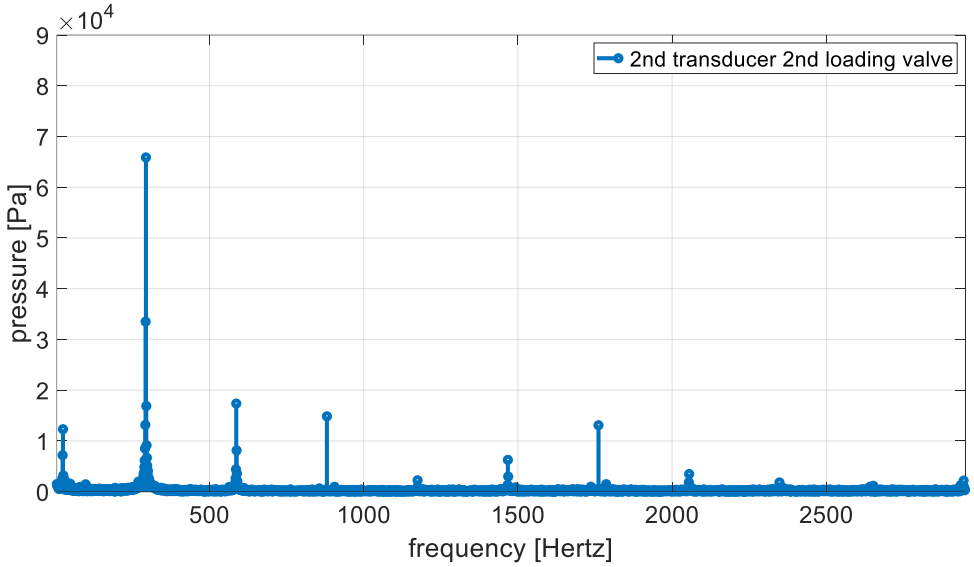

Figure 39 Transducer 2, system 2

The values of the source flow ripple of the first ten harmonics, computed using the Norton model are plotted in figure 40:

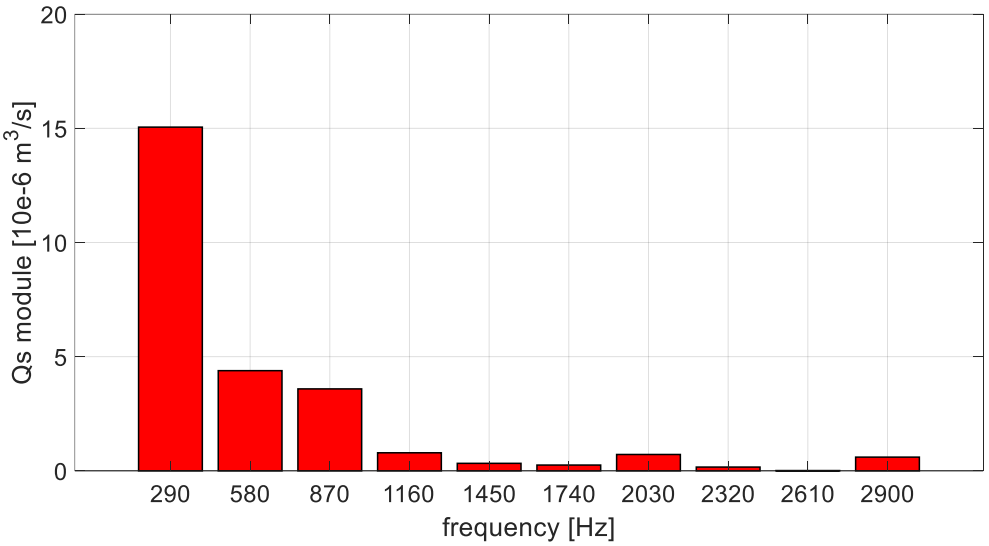

Figure 40 Module of the flow ripple computed with the Norton model

The experimental results present a peak at the fundamental harmonic equal to 0.9 lpm, while the following harmonics see a decrease of the module of more than three times. Thus, the hydraulic noise for this working condition is found to be, as expected, at the first harmonics. The results evaluated considering the source flow ripple located exactly at the outlet port of the pump are confirmed also considering its real position (“modified model”). But they differ in terms of amplitude, obtaining a peak value equal to 1.08 lpm and lower values in the following harmonics. Thus, it is possible to state that the pump at this condition has a good response in term of flow ripple, showing only one important peak.

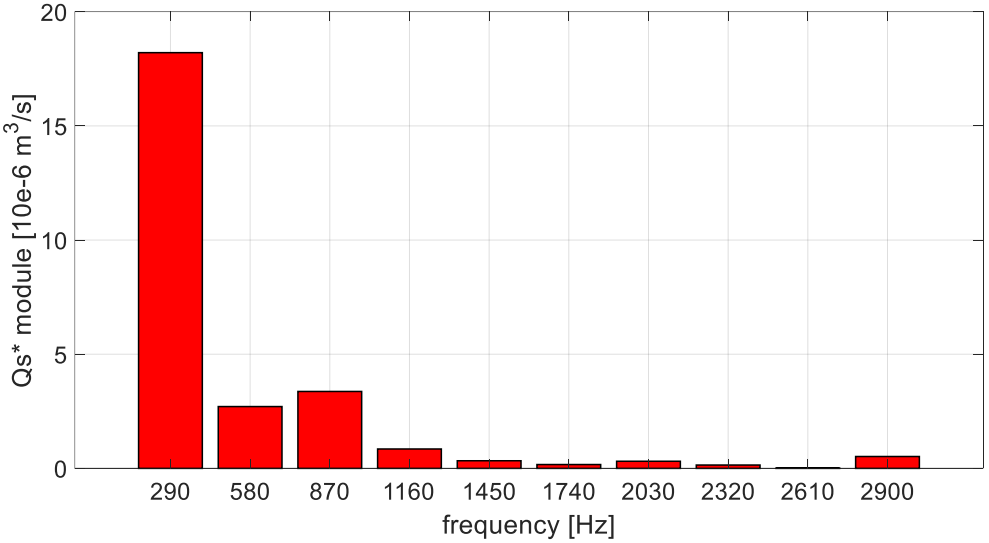

Figure 41 Module of flow ripple computed with the modified model

Moreover, the trend of the flow fluctuation is also plotted in time domain. At each cycle, there is one main fluctuation, accompanied by a minor one. The latter ones can be attributed to the contribution of the second and the third harmonic, while the fundamental harmonic generates the main peak. Moreover, compared to the theoretical curve, the experimental results are very reliable, having the same trend and the same amplitude.

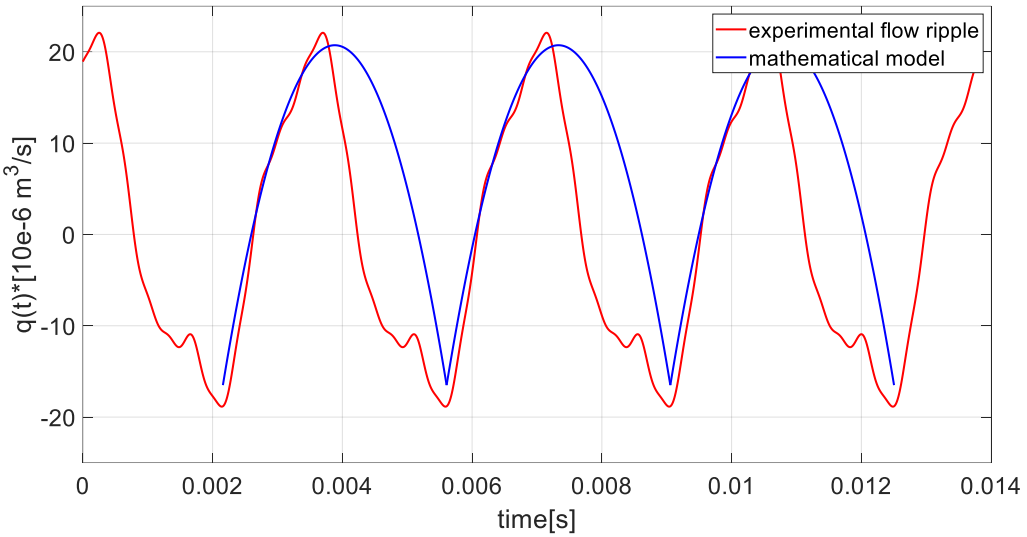

Figure 42 Comparison between the experimental and theorical time history wave form of pressure ripple

In figure 43 the module of the source impedance is plotted:

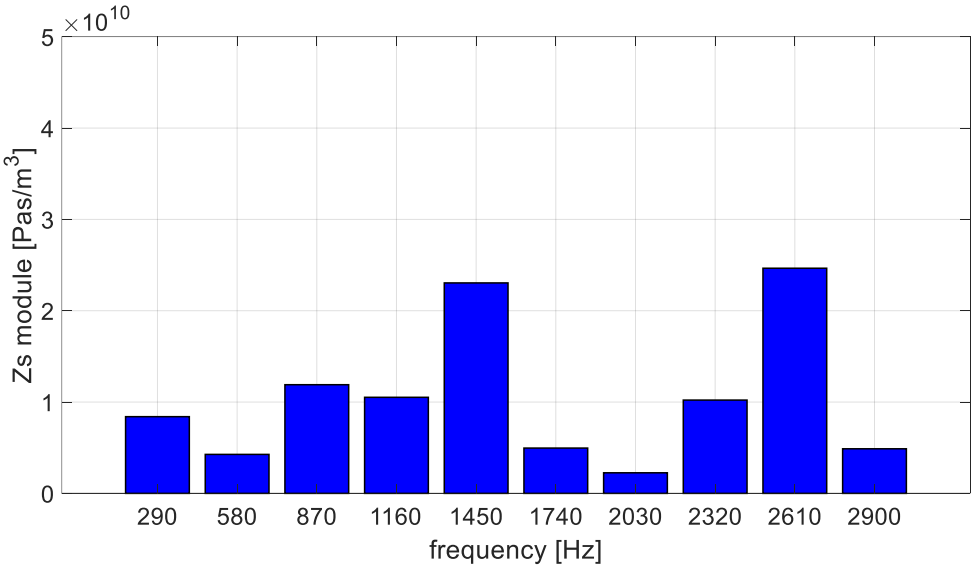

Figure 43 Module of the source impedance

The plot shows a not homogenous trend of the source impedance, which finds three main peaks at the third, the fifth and the ninth harmonic, the latter is the most important. These results show that the impedance of the pump has not a capacitive nature and additionally, comparing the experimental values with the two models, it is possible to state that for this operating condition the model that is closest to the evaluated results is the one computed using distributed parameters, even if a delay of the anti-resonance can be observed between the two curves. In fact, in the distributed parameter, model it occurs at 2030 Hz while in the experimental results it occurs at 2320 Hz, (one harmonic successive).

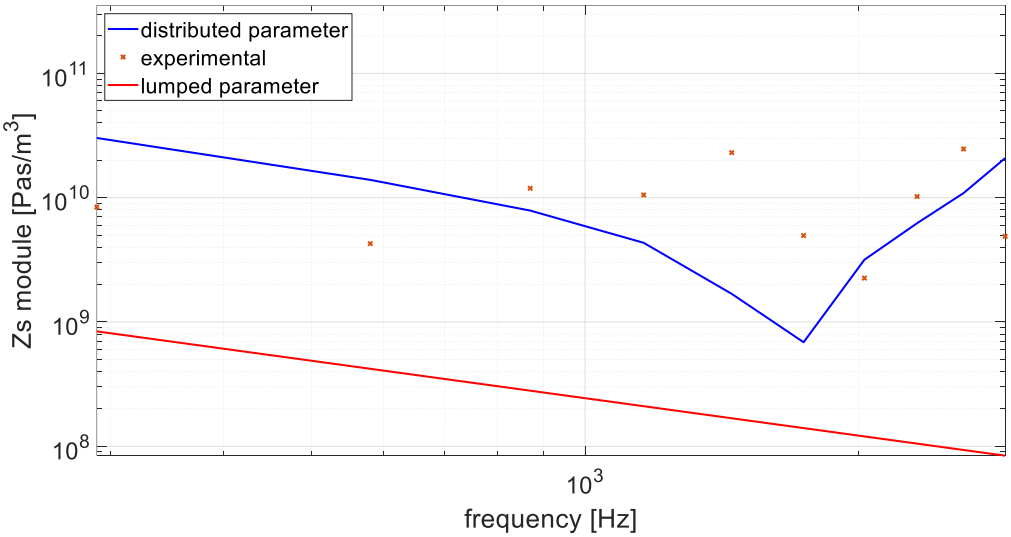

Figure 44 Comparison between experimental source impedance and mathematical models

Additionally, the blocked acoustic pressure is computed. Consequently, in case of an infinite entry impedance Z_e of the hydraulic circuit, a decreasing trend of the pressure is computed. It shows a peak of approximately 1.3 bar located at 290 Hz, while at the other frequencies the module is one order of magnitude lower. Moreover, the overall root mean square value is equal to 0.96 bar.

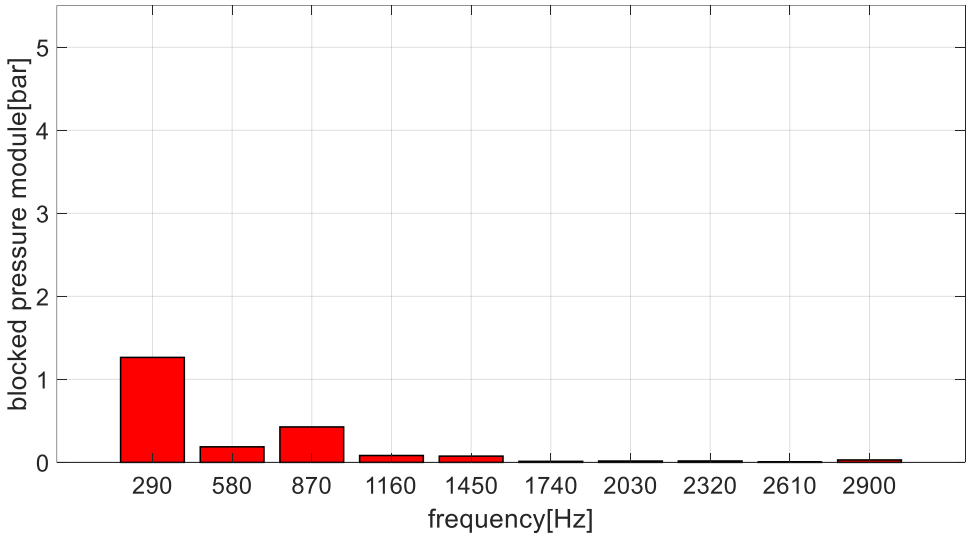

Figure 45 Module of blocked acoustic pressure

Finally, following the mathematical model suggested by Choi, Lee and Ji is evaluated the quality of the computed flow ripple source and the source impedance. We can state that the mathematical model and the experimental pressure fluctuations in the harmonic spectra show a good correlation among them.

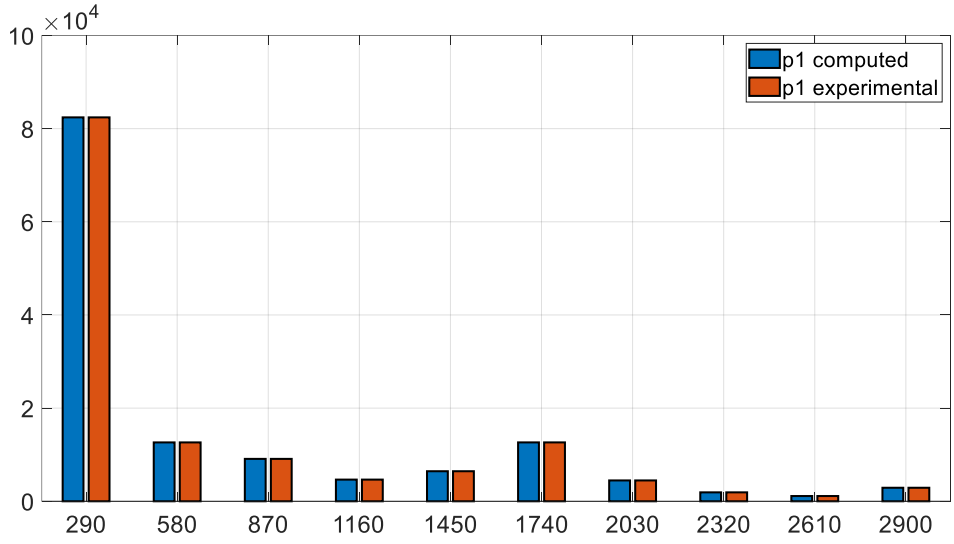

Figure 46 Comparison between experimental and computed pressure fluctuations in harmonic spectra

7.3.2 RESULTS AT 75 BAR

The second test is carried out at a load pressure of 75 bar and at a temperature equal to 35° C. The maximum pressure fluctuation in the time domain is equal to 3.7 bar measured in the first pressure transducer of system 1. While in the harmonic spectra the main contributions to the pressure ripple are equal to 0.85 bar and to 0.58 bar. They are located at the fundamental harmonic, respectively for the first transducer of the system 1 and for the first transducer of the system 2.
As in the previously test, the source flow ripple for the Norton and the modified model as well as the source impedance are computed for each harmonic.
The source impedance is plotted in figure 47 and shows a capacitive nature up to the fourth harmonic. In the fifth harmonic a peak is present, as well as in the ninth harmonic.

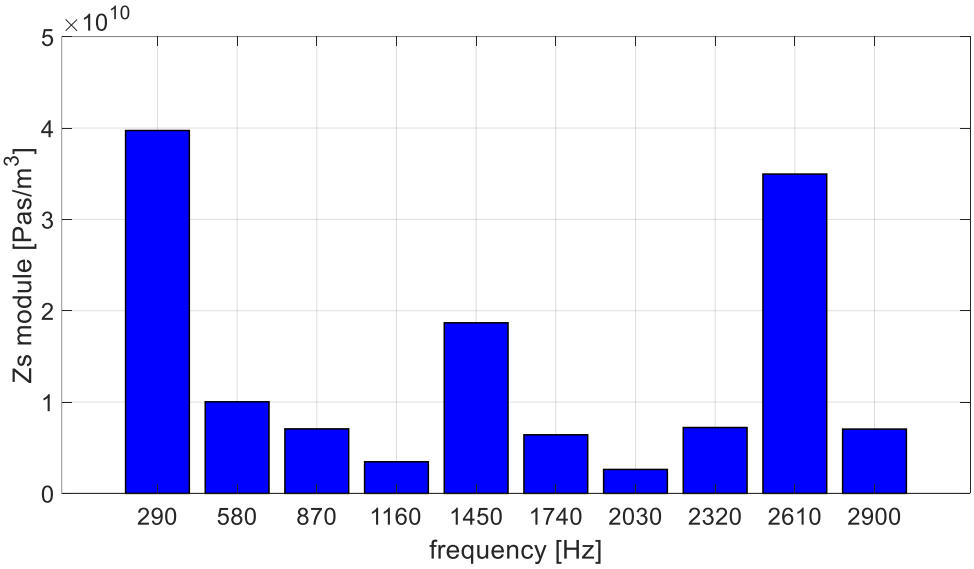

Figure 47 Zs module in frequency domain

In addition, if we take into consideration the mathematical models computed through lumped and distributed parameters, we can state that the experimental results and the distributed parameter model exhibit a good correspondence. With a main difference located at the fifth harmonic (1450 Hz) where instead of an anti-resonance is presents a resonance. Moreover, the anti-resonance shown in the mathematical model, occurs experimentally in the seventh harmonic, founding the same delay of the test carried out at 50 bar.

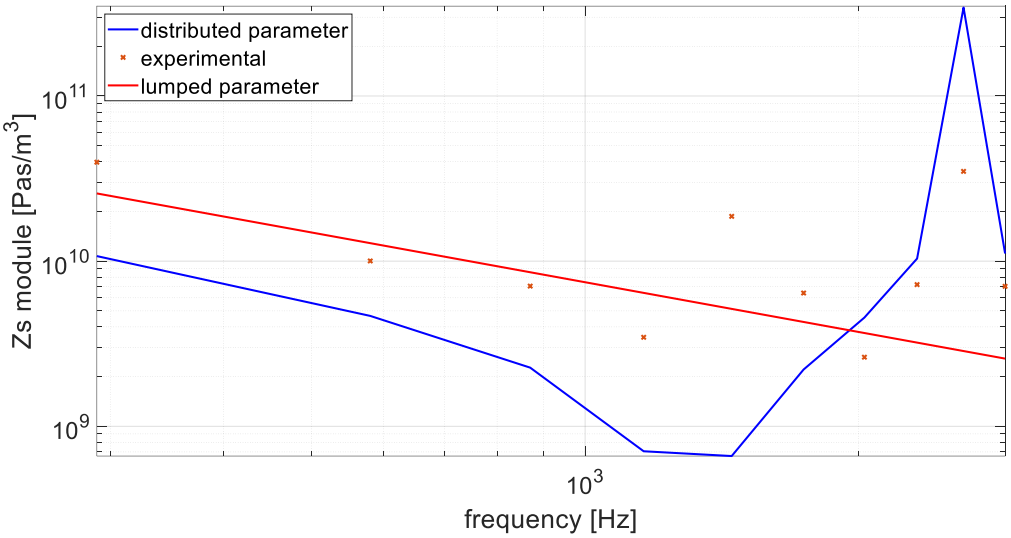

Figure 48 Comparison between source impedance computed and mathematical models

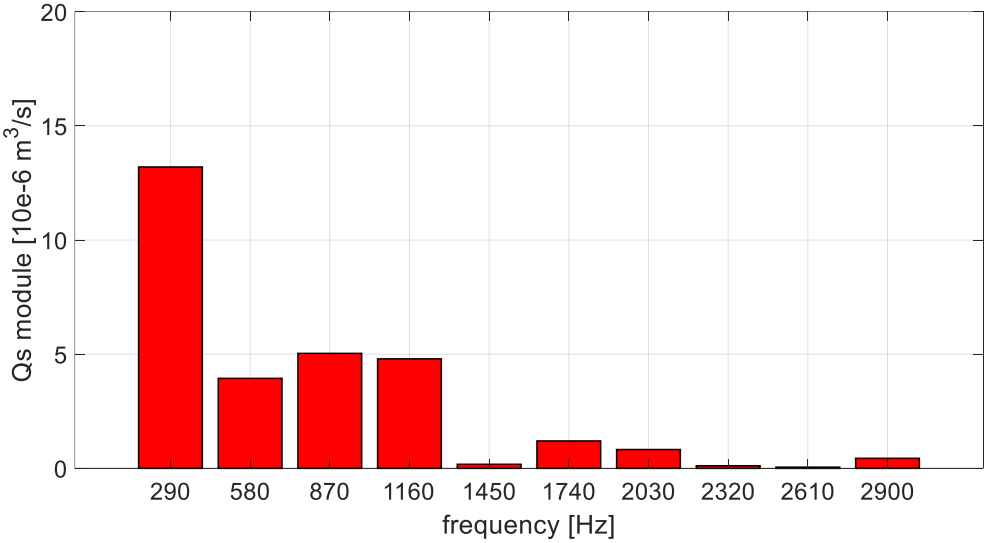

Figure 49 Module of flow ripple in Norton model representation in time domain

The experimental results remark the expected behaviour of external gear pumps. Therefore, having a peak in the first harmonic, which at 75 bar is almost equal to 0.8 lpm. And lower contributions which occur in the successive harmonics whose absolute values are three times lower respect the one corresponding to the fundamental harmonic. To have a more realistic representation of the source flow ripple, it is preferable to compute it with the modified model and so also considering the fluctuations which occurs in the inner part of the discharge line.

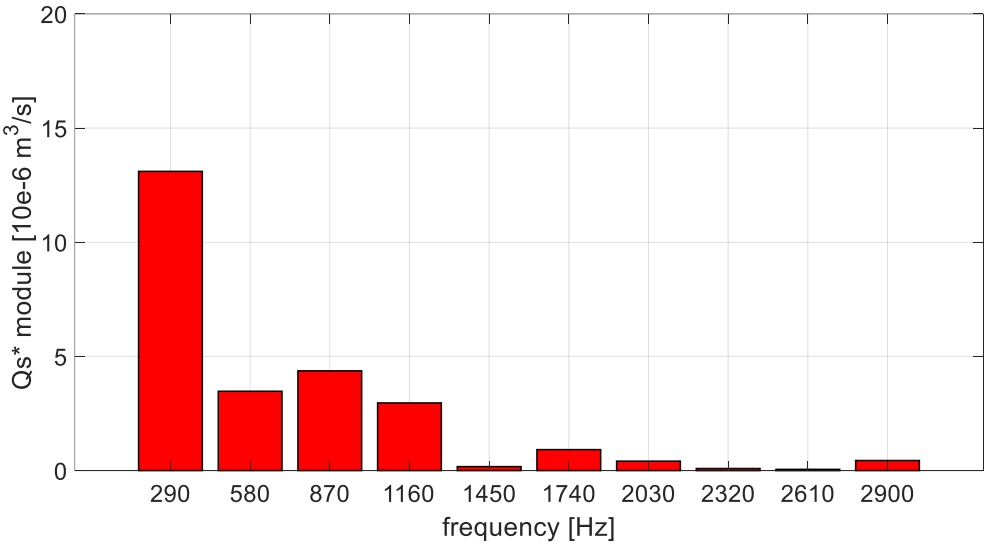

Figure 50 Module of flow ripple in modified model representation in time domain

The main difference between the two models is found in the second, the third and the fourth harmonic, where the module of the flow fluctuations decreases. Generally speaking, the two models follow the same decreasing trend, remarking so the good design of the hydraulic pump, having found only a significative peak in the first harmonic.
Moreover, figure 51 compares the time history wave form computed experimentally and through the theorical model. As well as in the previous test, the experimental results are validated. In fact, the two curves have the same trend, even if the experimental one does not follow perfectly the theorical inverted parabola, presenting two additional peaks, that can be attributed to range of frequencies between 580 Hz and 1160 Hz.

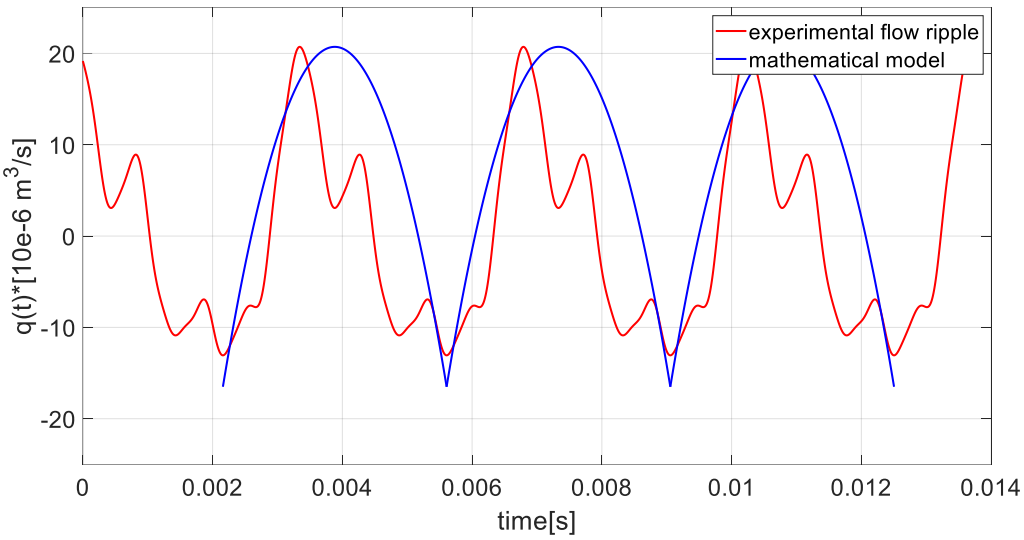

Figure 51 Flow fluctuations in time domain

Furthermore, an important characteristic to be evaluated is the blocked acoustic pressure, which is shown in figure 52.

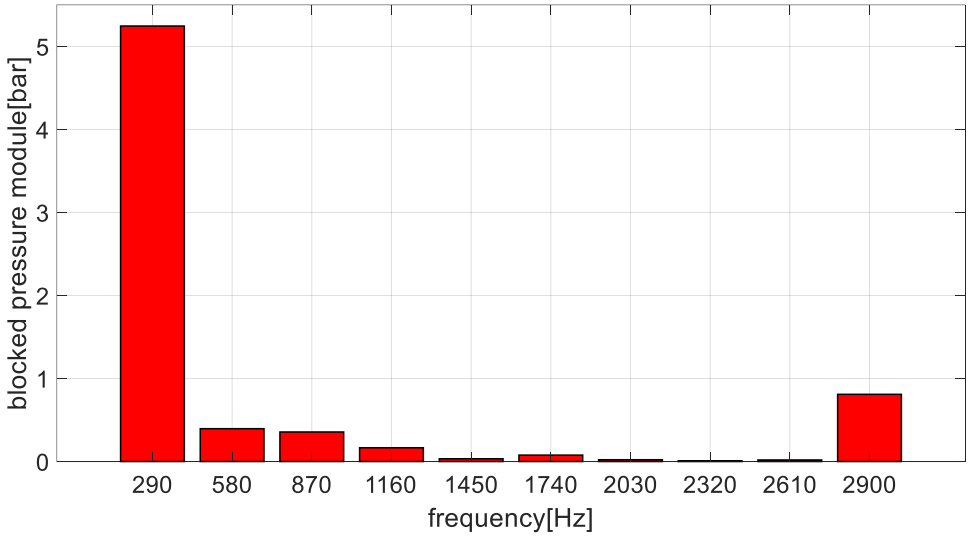

Figure 52 Blocked acoustic pressure in frequency domain

The maximum peak is located at the fundamental harmonic where is found a value of more than 5 bar, while the other harmonics show irrelevant contributions. The overall root mean square value is equal to 3.77 bar.

Finally, to evaluate the experimental results obtained, the pressures of the second transducer in system 1 are computed using the characteristic values. Later they are compared with the ones sampled through the digital scope.

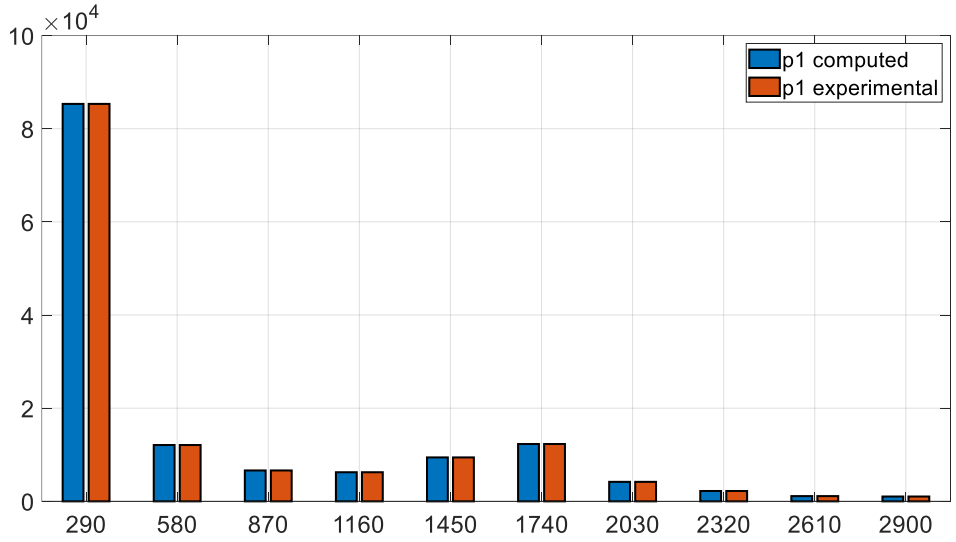

Figure 53 Comparison between experimental and computed pressure fluctuations in harmonic spectra

7.3.3 RESULTS AT 90 BAR

In the last test a mean working pressure of 90 bar is used, while the fluid temperature is equal to 45°C.
The results in term of source impedance remark the ones computed at 50 bar. As the figure 54 shows, the pump impedance exhibits two peaks at 1450 Hz and at 2610 Hz. Consequently, if up to 1KHz it has a capacitive nature, from the fourth harmonic the inertia of the working fluid cannot be neglected, showing an inductive nature.

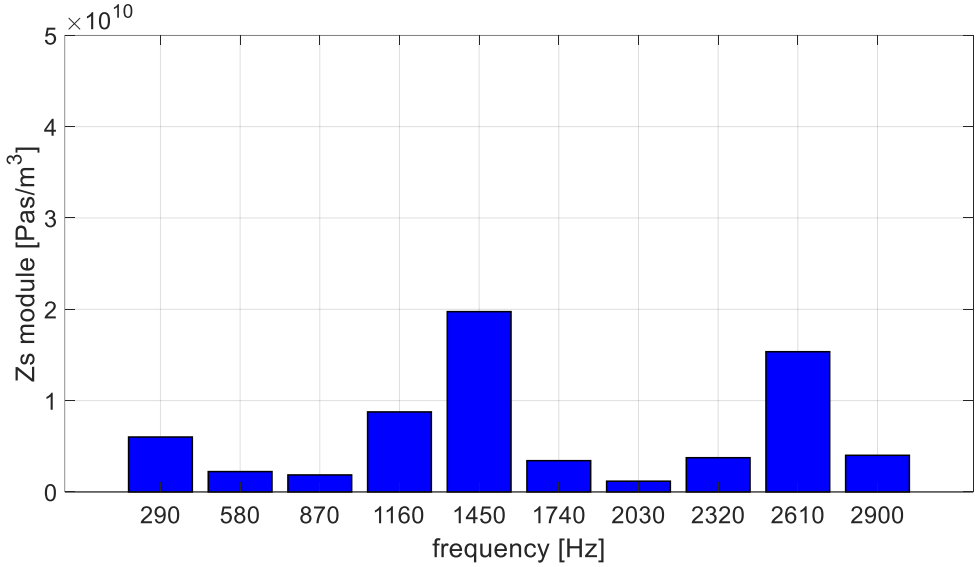

Figure 54 Module of source impedance in harmonic spectra

The distributed parameter model and the experimental points show a good correlation, even if where the mathematical model presents an anti-resonance, the empirical results exhibit a resonance. This one is accompanied by an anti-resonance located at the seventh harmonic (2030 Hz), expressing the same delay occurred in the previously tests.

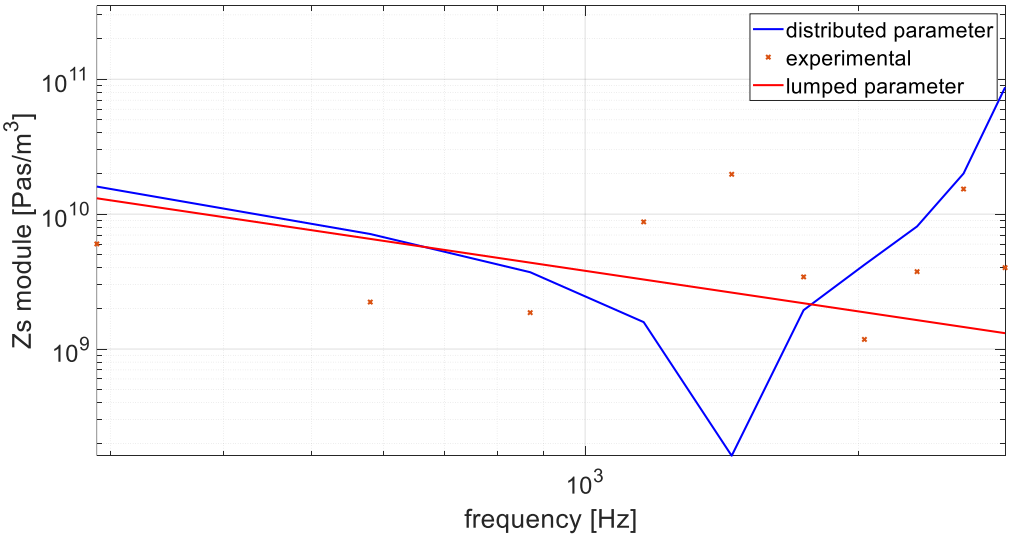

Figure 55 Comparison between experimental results of source impedance and mathematical models

Regarding the flow ripple evaluated using the Norton model, as in the test carried out at 75 bar, it exhibits a peak of almost 0.8 lpm at 290 Hz, while the second harmonic shows a halved value respect to the fundamental one. Furthermore, also at 870 Hz an important contribution is found, exhibiting a wider range of hydraulic noise respect the test at 50 bar.

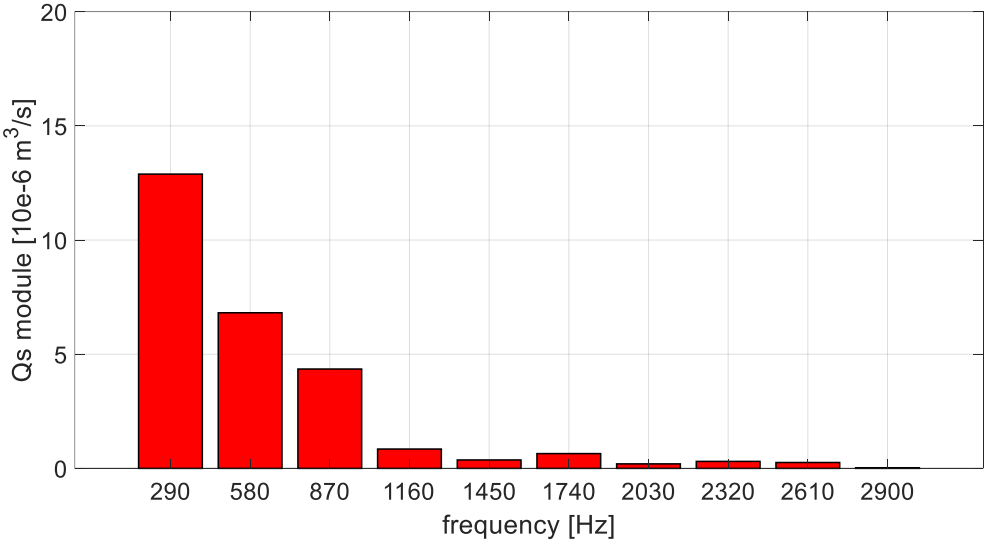

Figure 56 Module of flow ripple source (Norton model)

When the modified model is used, a better behaviour of the pump is exhibited. Even if the main contribution is almost unchanged (0.7 lpm respect to 0.8 lpm), the following harmonics show a large decrease, having values with one order of magnitude lower respect the fundamental harmonic.

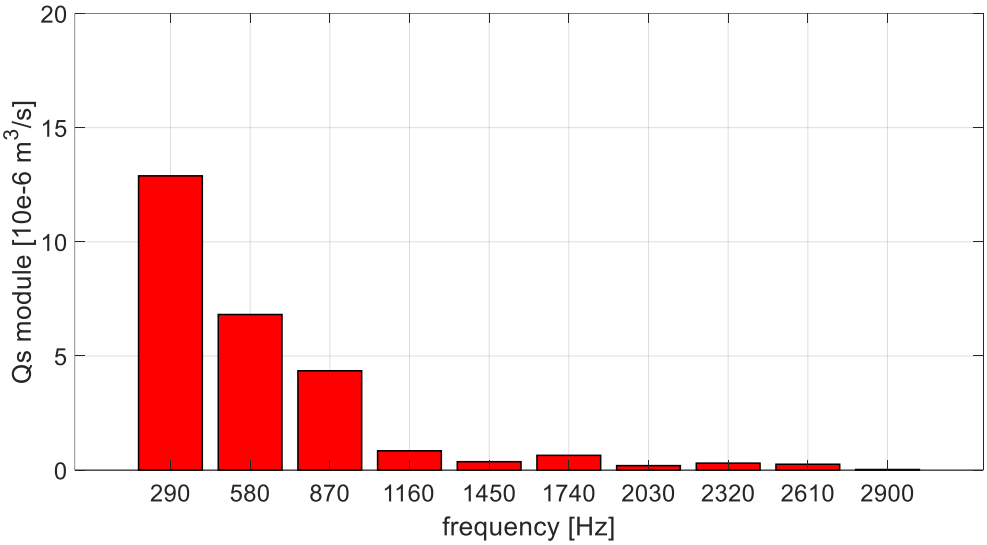

Figure 57 Module of flow ripple source (modified model)

Furthermore, the fluctuations in time domain reflect the ones found at 50 bar, with the main peak belonging to the first harmonic and very small deflections respect to the theorical inverted parabola. The only difference with the mathematical model consists in the range of amplitude where the two curves lie. If for the model is between 20 and $-20 \cdot 10^{-6}$ m^3/s, for the empirical results it is between 10 and $-15 \cdot 10^{-6}$ m^3/s.

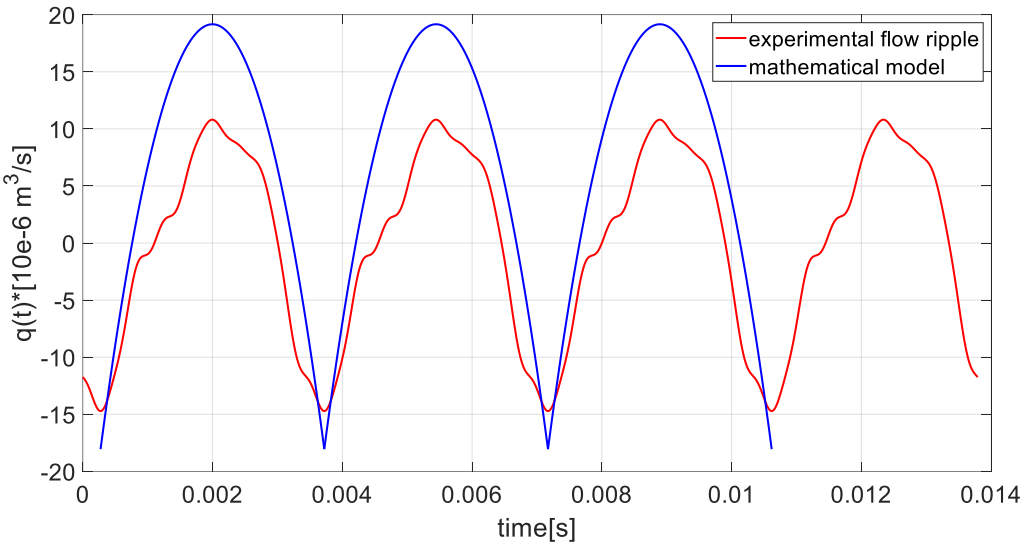

Figure 58 Flow ripple fluctuations in time domain

Moreover, respect to the other tests, the blocked acoustic pressure presents lower values at both the fundamental and the other harmonics. In addition, the overall root mean square value is equal to 0.57 bar.

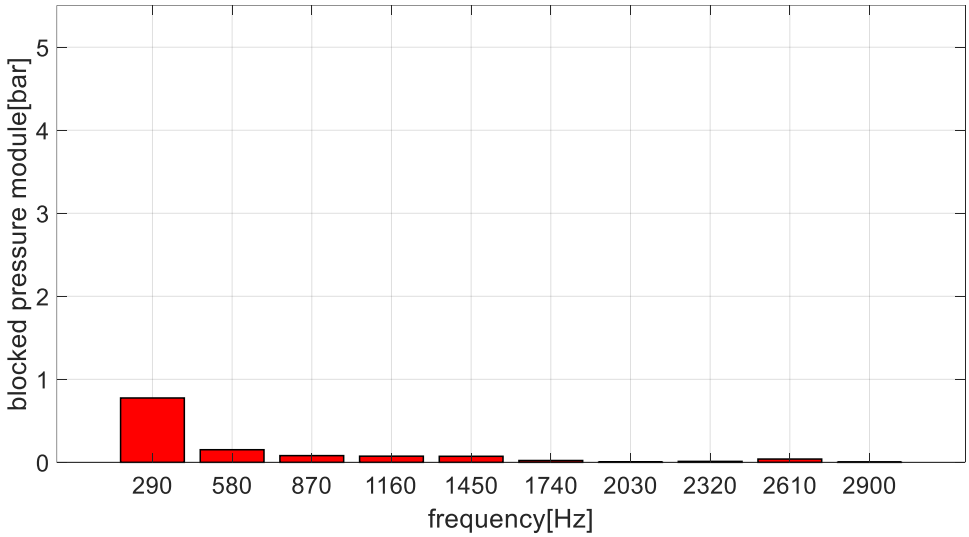

Figure 59 Blocked acoustic pressure

To sum up, as well for the other test, a comparison between the pressure fluctuation of the second pressure transducer in system 1 is made. Also in this test, a good correlation between the model and the experimental results is found, stating thus, the quality of the Norton and the modified model.

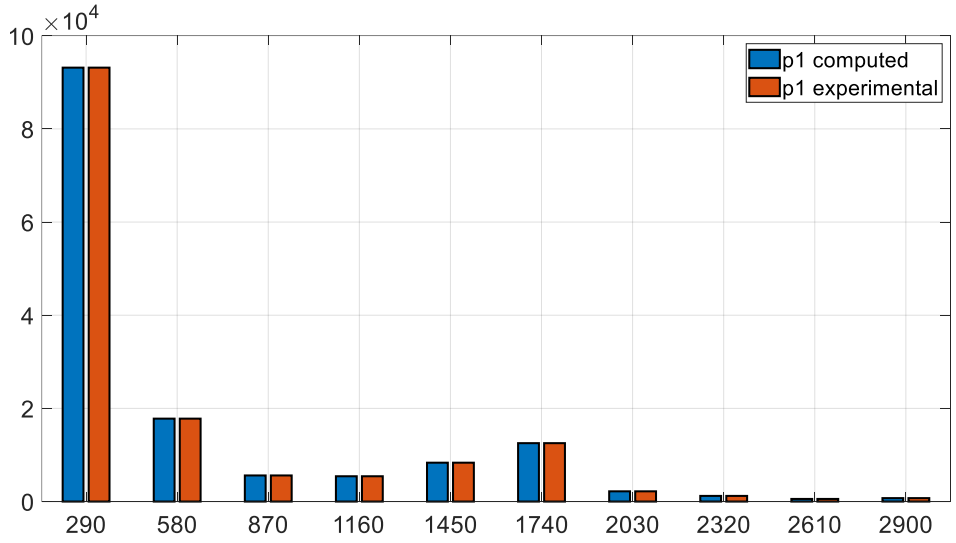

Figure 60 Comparison between pressure fluctuation of 2nd pressure transducer of system 1

7.4 COMPARISON AMONG THE EXPERIMENTAL RESULTS

As explained in chapter 2, the source impedance of a hydraulic pump is a function of the geometry of the pump, its volumetric efficiency, working fluid's property and the possibility of occurrence of cavitation or liberation of air in the hydraulic circuit. Therefore, it should be invariant changing the loading pressure.
As seen in the different tests, the pump impedance follows the same trend, having a capacitive nature in the first harmonics, while starting from 1450 Hz the inertia of the fluid cannot be ignored, leading to an increment of its amplitude. At every working condition an anti-resonance is observed at the eight harmonic (2320 Hz), followed by a resonance located at the ninth harmonic. Furthermore, the trend of the source flow ripple, computed both with the Norton and the modified model, shows how the positive displacement pump analyzed has an optimal design. It has only one significative hydraulic noise at the pumping frequency and unappreciable values at the following harmonics. Moreover, it is important to state that among them, the results show a good repeatability even if regarding the blocked acoustic pressure a significative difference is present in the test carried out at 75 bar. Here it is reached a peak of more than 5 bar while at 50 bar and at 90 bar the highest values are respectively 1.3 bar and almost 0.8 bar. In addition, also the trend of the source impedance's amplitude slightly differs from the other tests. A more capacitive nature is exhibited, without showing a remarked resonance at the fifth harmonic (1450 Hz) as for the other tests.
Generally speaking, the experimental results are confirmed by the theoretical models. The source impedance computed in all the three tests shows a good correspondence especially at low and high frequencies, while between the fourth and the sixth harmonic a significative difference is encountered. Furthermore, being the distributed parameter model the one closest to the computed results, we can affirm that the dimension of the discharge port of the pump is similar to the wavelength of the signal analyzed. Finally, the values and the tendency of the pressure ripple in the spectra harmonic among the different tests are very similar, leading to very small difference about the hydraulic noise between the three loading conditions.
To sum up it is possible to state that the external gear pump analyzed has a useful design in terms of hydraulic noise. In fact, it respects the criteria for which this type of pumps

presents only one main peak of flow fluctuation located at the fundamental harmonic, while the other contributions are unappreciable.

CHAPTER 8

RESULTS AND COMPARISON

In this chapter the results achieved in the three tests are compared with scientific articles. It is important to remark that the methodologies and the types of positive-displacement pumps analyzed in the articles in some cases differ respect the ones addressed in this thesis.

8.1 COMPARISON WITH THE ARTICLE "DEVELOPMENT OF STANDARD TESTING PROCEDURE FOR EXPERIMENTALLY DETERMINING INHERENT SOURCE PULSATION POWER GENERATED BY HYDRAULIC PUMP"

The first comparison is made with the article "DEVELOPMENT OF STANDARD TESTING PROCEDURE FOR EXPERIMENTALLY DETERMINING INHERENT SOURCE PULSATION POWER GENERATED BY HYDRAULIC PUMP" written by Eiichi Kojima, Toru Yamazaki and Kevin Edge [10].
Here an axial piston pump is analyzed following the two systems two pressures method. Being an axial piston pump, its behaviour is a bit different from the one that we have analyzed since the external conditions cannot be neglected for the computation of the flow ripple. Moreover, in this article the characteristic values of the pump are computed up to seventeenth harmonic while in our study up to the tenth.
Nevertheless, the results obtained regarding the source flow ripple are very similar. A decreasing trend is found in the first tenth harmonic, as well as in our experimental data. Furthermore, also the order of magnitude shows a good correlation.

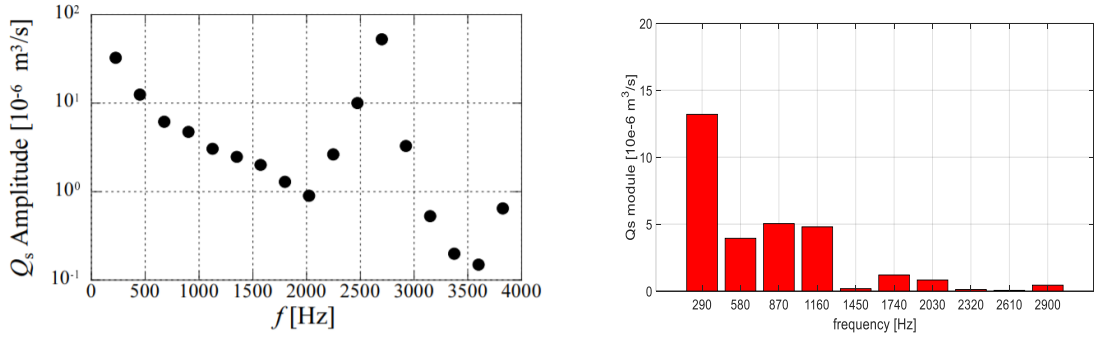

Figure 61 Comparison between source flow ripple (Norton model)

About the source impedance, for the axial pump a capacitive nature is found up to the twelfth harmonic with an increasing trend for the successive harmonics. This behaviour is very close to the one showed by our pump at the working condition of 75 bar. In fact, we found a resonance at the ninth harmonic while an anti-resonance at the seventh harmonic. These little differences can be attributed to the different working conditions as well as to the different geometry of the pump. Furthermore, the order of magnitude between the two studies exhibits a good correspondence.

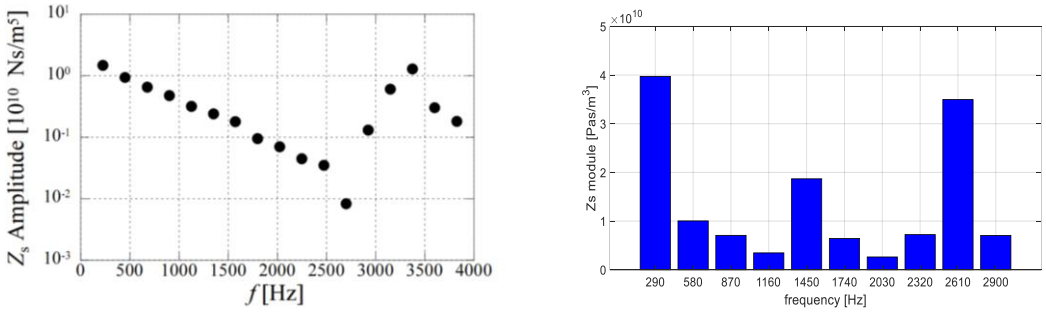

Figure 62 Comparison between source impedance

8.2 COMPARISON WITH THE ARTICLE "THE TEMPARATURE CHARACTERISTICS OF FLOW RIPPLE AND SOURCE IMPEDANCE IN AN EXTERNAL GEAR PUMP"

Moreover, our pump is also compared with an external gear pump which differs from our for the number of teeth (10) and the displacement capacity (30 cc/rev).
In the article "THE TEMPARATURE CHARACTERISTICS OF FLOW RIPPLE AND SOURCE IMPEDANCE IN AN EXTERNAL GEAR PUMP" written by ICHIYANAGI, NISHIUMI and NAKAGAWA [11] the working condition used for the test are close to ours, making their results a good reference for us.
For example, the type of hydraulic oil is the same as well as the working temperature. But little differences are present in term of mean pressure (100 bar) and rotational speed of the pump (900 rpm). However, the results show a similar behaviour for both the characteristic values and the time history wave form of the flow ripple.
In figure 63 we can see that for the 30 cc/rev pump it is found a peak of source flow ripple at the fundamental harmonic and less significative harmonics, whose the most important is the third one. In our computations made at 75 bar, the trend of the modified model source flow ripple reflects the one of the 30 cc/rev pump.

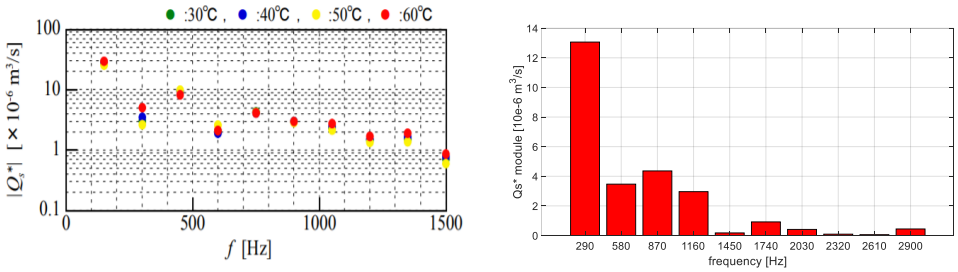

Figure 63 Comparison between source flow ripple (Modified model)

In addition, the flow ripples in the time domain computed at the inner section of the discharge port of the pump are very close among them.

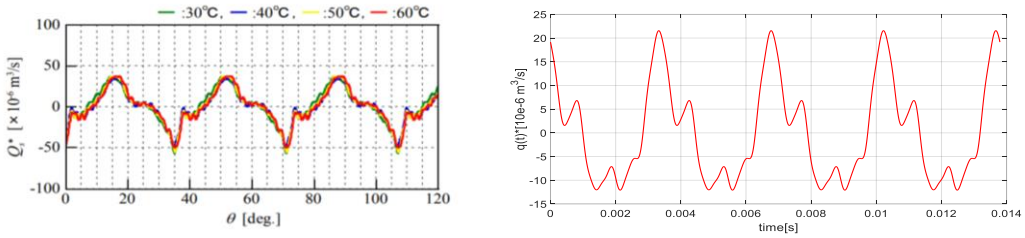

Figure 64 Comparison between flow fluctuations in time

Finally, the source impedance is compared. Figure 65 shows a capacitive nature for the 30 cc/rev pump, without any presence of resonance as found in our study. That could be attributed to the fact that it is expected at higher harmonics than the tenth.

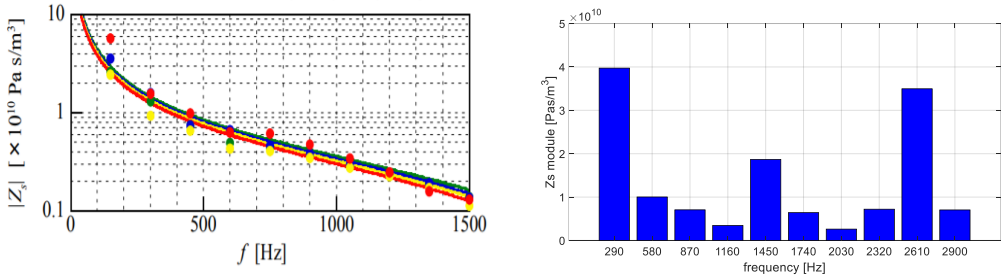

Figure 65 Comparison between source impedance

8.3 COMPARISON WITH THE ARTICLE "MEASURMENT OF FLOW RIPPLE IN POSITIVE DISPLACEMENT PUMPS"

If in the previous comparisons the source impedance showed a good correspondence with the one computed at 75 bar. In the article "Measurement of Flow Ripple in Positive Displacement pumps" [9] the characteristic values are very close to the one found at 50 bar and 90 bar. In this article an axial piston pump is studied using a slightly different approach respect to the two systems two pressures. As it is possible to see in figure 66 the source impedance has two significative resonances, one in the middle range of harmonics and the other at the ninth harmonic as in our experimental results.

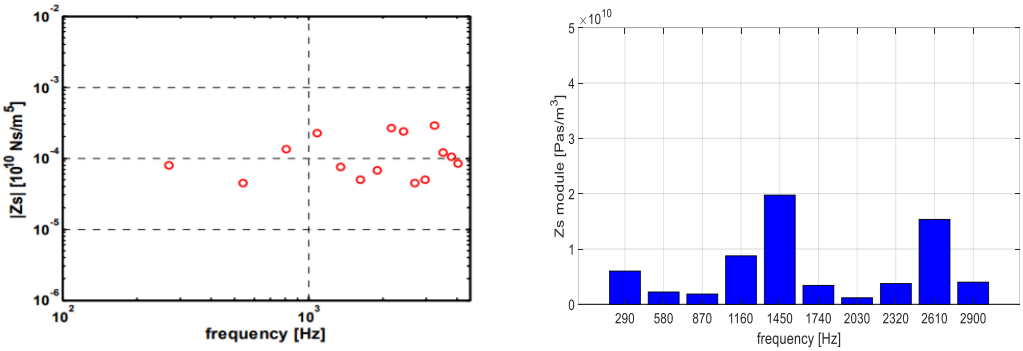

Figure 66 Source impedance comparison

In addition, the behaviour of the source flow ripple is also very close among our methodology and the one followed by CHOI. The curve has only one significative peak followed by less important harmonics.

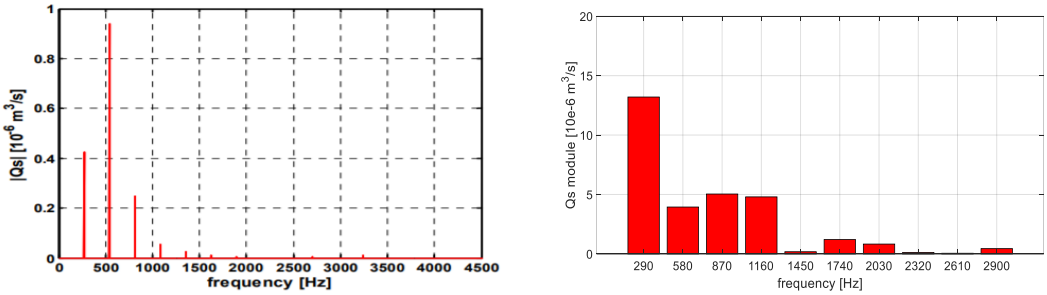

Figure 67 Source flow ripple comparison

8.4 COMPARISON WITH THE THESIS “MEASUREMENT AND PREDICTION OF THE FLUID BORNE NOISE CHARACTERISTICS OF HYDRAULIC COMPONENTS AND SYSTEMS”

Finally, considering that our methodology is based on the ISO 10767:2015 it is interesting making a comparison with the older version of the same standard. About this, the studies of Johnston [2] are taken into account. Here it is studied an external gear pump having the same number of teeth of the one tested by us, but with higher volumetric capacity (16.1 cm^3/rev).
The source impedance shows a capacitive nature, followed by the presence of a resonance at the higher harmonics. This behaviour is very close to the one computed at 75 bar.

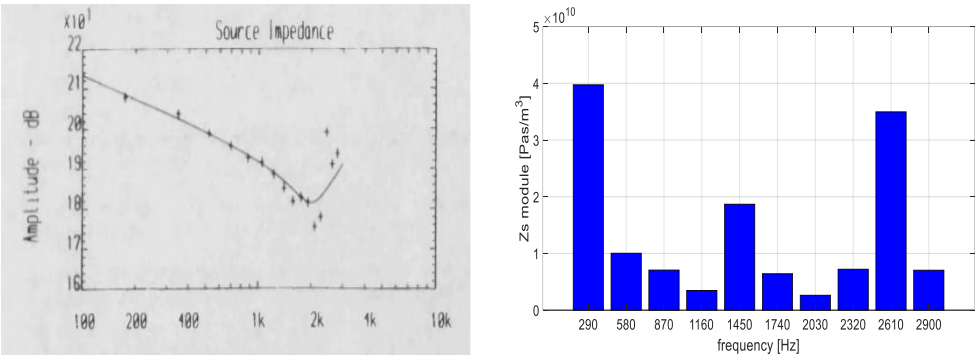

Figure 68 Source impedance comparison

Moreover, the source flow ripple is very close to our experimental results, both in term of amplitude and in term of wave form time history.

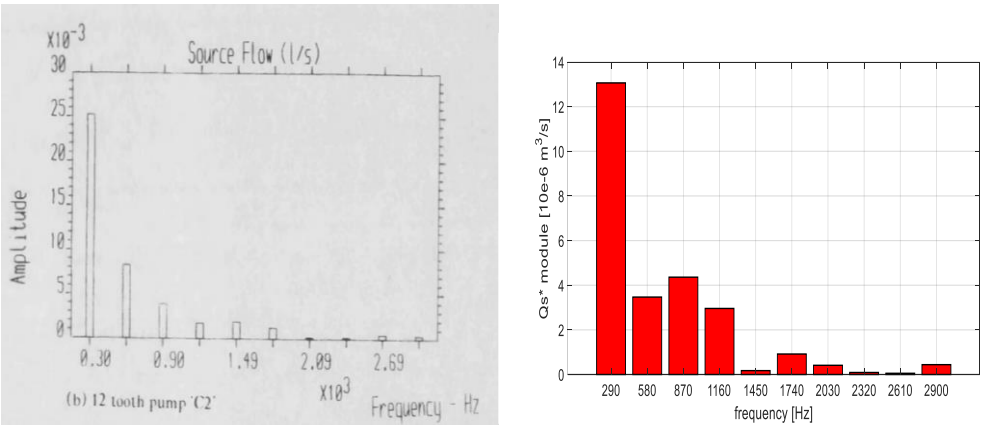

Figure 69 Source flow ripple comparison

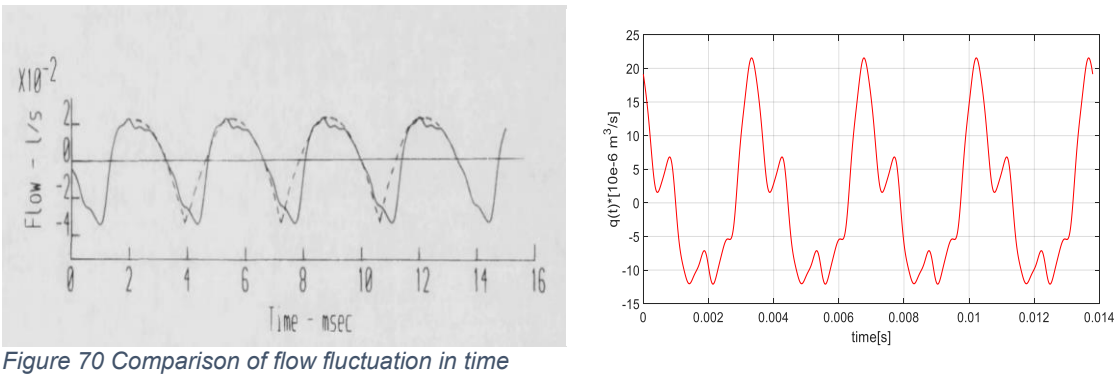

Figure 70 Comparison of flow fluctuation in time

8.5 SUMMARY OF COMPARISON

To sum up, we can state that the complete characterization of the pump studied finds a good correspondence with different scientific articles, whether they follow the same computational methodology or slightly different. Consequently, we can affirm that even if we have used typical instrumentation of a university instead of high technology equipment, the experimental results achieved are reliable and could be very useful to improve the noise production of the hydraulic circuits mounted in our laboratory.

CHAPTER 9

9.1 BUDGET

The thesis has been developed over the course of five months and different typologies of costs should be taken into account. We divide the costs into two main categories, direct and indirect. To sum up an overall cost of 16133.54€ should be considered for the realization of this thesis.

9.2 ECONOMIC VIABILITY

It is important to state that almost the 70% of the hours spent for this thesis are attributed to learn the methodology, writing the code and the installation of the test bench. In addition, most of the costs belongs to initial expenses of the instrumentation and in the working hours dedicated by the laboratory staff. Therefore, once becoming familiar and having carried out the first tests, the cost of further positive displacement pump studies will be significantly lower.
For this reason, due to the importance of characterizing positive displacement pumps and to the fact that the cost could be amortized during the year the decision to implement this test in the laboratory of UPC university could be considered a feasible and sensible decision.

CHAPTER 10

ENVIRONMENTAL ANALYSIS

During the development of this thesis, we have always taken into account how to improve our environmental impact. At this regard, during the theoretical study the use of notebooks and paper sheets was avoided and was replaced by a tablet. In addition, the experimental part was carried out in the morning, thus there was no need of an artificial lighting.
Furthermore, during the tests it is estimated a power consumption of 128 kWh. Therefore, it is possible to convert the power consumption into Carbon dioxide and equivalent gasses emission to have a better vision of the environmental impact.

kWh	Emission of CO_2 [kg]
128	**29.842**

Table 21 CO2 emission

For our test, an emission equal to 29.842 kg of CO_2 is found [12]. This value corresponds to the consumption of 11.3 liters of diesel or 12.37 liters of petrol.
Furthermore, considering a daily consumption of 4.6 kWh per household, we can affirm that our tests have consumed the same amount of energy of a family for 28 days.
In addition, during the tests the Renoil B10 hydraulic oil was used. Due to its improved lifetime, it can be used for a long period. It is important to know that hydraulic oil is classified as a hazardous waste. Consequently, at the end of its life it has to be treated in the correct way. Otherwise, it can damage the environment.
Hydraulic oil can be subjected to different treatments.

- **Energy recuperation**,
  After a chemical treatment, the used oil can be suitable for being used as a fuel in industrial plants. Thanks to its high heating value 1 litre of oil can provide more than 10 kWh.
- **Regeneration**,
  During its working life, the industrial oil is contaminated by different materials such as metals, additives or also water. If the oil is cleaned up with chemical treatments, it can be reintroduced in the working area. The quality and the effectiveness of this type of treatment is significative. The yield of the regeneration is up to 70 %.
- **Recycling**,
  Used oil cannot also be used to produce other types of materials.

Furthermore, during the test the standard ISO 15380 is followed. Therefore, we impose 2% as the maximum contamination threshold. In addition, it would be interesting the adoption of biodegradable oil instead of mineral one. In this way, the environmental impact would be further reduced.
To sum up, during this thesis an intelligent use of electrical resources was made, trying to limit any environmental impact as much as possible.

CONCLUSION

This thesis concerns the study of positive-displacement pumps in terms of source flow ripple and source impedance. To achieve these results a preliminary theoretical study of the flow fluctuations and of the standing wave propagation in hydraulic pipes was mandatory. Moreover, in chapter 4 a comparison between the old and the new version of the standard ISO 10767:1 has been furnished, making clear advantages and disadvantages of the 2015 version and the reasons for choosing it.

During the development of this work, a test bench suitable for the characterization of positive-displacement pumps has been designed. Since it is equipped with three kits, it is suitable for a wide range of hydraulic pumps.

Furthermore, following the standard ISO 10767:1-2015, a Matlab code was written. Its functions are to compute the source flow ripple and the source impedance. In addition, it provides an example of the evaluation of the pressure ripple in a hydraulic circuit. Considering an infinite entry impedance, the blocked acoustic pressure is computed. Moreover, the code provides different comparisons of the experimental results with theorical models.

Finally, in the experimental section of this thesis, a direct proof of the correctness of the methodology followed for the design of the test bench and of the code is provided. This is achieved by testing a 10.6 cc/rev external gear pump at different working pressure, 50, 75 and 90 bar.

The tests have been carried out in different days, reporting not only repeatability of the results but also consistency with different mathematical models.

The experimental source flow ripple obtained with both the Norton model and with the modified one shows the typical behaviour of external gear pumps having a strong harmonic at the pumping frequency and smaller harmonics at higher frequencies.

On the other hand, the source impedance shows a good correspondence with the distributed parameter model. Therefore, it can be stated that the methodology to design the test bench and the code written for the computation of the characteristic values are reliable.

Furthermore, with this thesis, the knowledge I have acquired was multidisciplinary. Different engineering topics have been covered. Regarding the mechanical field, I remember mechanical drawings and fluid mechanics studies. On the other hand, by writing a Matlab code I have raised my level in the IT field. Finally, for the first time in my academic career I have made use of high complexity instrumentation such as the digital scope.

In addition, it is important to state that during these months, I have improved some of my soft skills. For example, during the experimental section, different problems have arisen. Therefore, after working rigorously I have been able to achieve the expected results. In this way I have also understood how little errors can influence the physic of the problem faced.

Moreover, this thesis provides an important laboratory practice to the future students of the UPC University, making possible to understand in a more practical way the flow ripple generation in positive-displacement pumps. To sum up, this thesis can also be exploited by the CATmech. Through the methodology and the code I have furnished, it is possible to offer standardized tests to private companies.

FUTURE WORKS

Having designed a test bench suitable for different positive-displacement pumps, the next step is its installation in the Laboratory of Fluid Mechanics of the UPC University. Moreover, having already tested an external gear pump, it would be interesting testing other type of external gear pumps so that the influence of the geometry could be better understood. Furthermore, also the dependence of the rotational speed could be a useful parameter to consider. In addition, further works could be focused on the study of axial piston pumps so that a direct comparison of the two types of machines could be done.

As previously specified, the aim of the knowledge of the parameter we have computed is the computation of pressure ripple inside hydraulic circuits. Therefore, it would be very interesting to continue our work characterizing all the components of the circuit as explained in the standard ISO 15086-3 [13]. In this way by making use of software, it would be possible to compute the pressure fluctuations in the circuit.

Finally, since the real part of the source impedance is correlate to the fluid leakages, another interesting work could be relating the results obtained experimentally with the ones of the standard ISO 4409 [14].

Bibliography

[1] SAE, “STANDARD SAE J744”.

[2] N. J. David, "Measurement and prediction of the fluid borne noise characteristics of hydraulic," pp. 9-13, 1987.

[3] K. Edge, "The use of plane wave theory in the modelling of pressure ripples in hydraulic systems," School of Engineering, University of Bath, 1983.

[4] E. K.A., "The Theoretical Prediction of the Impedance of Positive Displacement Pumps," in *I. Mechanical E. seminar*, London, 1980.

[5] D. L.C., "The Internal Impedance of Centrifugal and Positive Displacement Pumps," in *A.S.M.E.* , Atlanta, 1977.

[6] I. STANDARD, "ISO 10767:1-1996". SWITZERLAND 1996.

[7] ISO, "10767-1:2015," 2015.

[8] ISO, "10767-1:1996," p. 14, 1996.

[9] L. J. Choi, "Measurement of Flow Ripple in Positive Displacement pumps (Effect of Approximation Model of Discharge passage in Pump)," *The 10th JFPS International Symposium on Fluid Power 2017,* 2017.

[10] T. Y. a. K. E. Eiichi Kojima, "DEVELOPMENT OF STANDARD TESTING PROCEDURE FOR EXPERIMENTALLY DETERMINING INHERENT SOURCE PULSATION POWER GENERATED BY HYDRAULIC PUMP," *International Journal of Fluid Power,* 2009.

[11] N. a. N. ICHIYANAGI, "THE TEMPARATURE CHARACTERISTICS OF FLOW RIPPLE AND SOURCE IMPEDANCE IN AN EXTERNAL GEAR PUMP," *The 10th JFPS International Symposium on Fluid Power,* 2017.

[12] [Online]. Available: https://www.rensmart.com/Calculators/KWH-to-CO2. [Accessed 07 06 2021].

[13] "Standard ISO 15086-3".

[14] "Standard ISO 4409".